Fire Retardant Caused Corrosion

AN INVESTIGATION

OF

FIRE RETARDANT CAUSED CORROSION

Final Report

to

UNITED STATES DEPARTMENT OF AGRICULTURE
FOREST SERVICE
INTERMOUNTAIN FOREST & RANGE EXPERIMENT STATION

A report of research performed under the auspices of the Intermountain Forest and Range Experiment Station, Ogden, Utah.

FOREST SERVICE
U S
DEPARTMENT OF AGRICULTURE

OCEAN CITY RESEARCH

OCEAN CITY, N.J. 08226
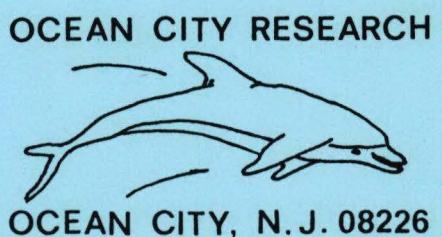
AN INVESTIGATION OF FIRE RETARDANT CAUSED CORROSION

FINAL REPORT
BY
G. A. Gehring Jr.

Contract 26 – 3250

30 September 1974

Intermountain Forest & Range Experiment Station

USDA Forest Service

Ogden, Utah 84401

Ocean City Research Corporation

Tennesse Ave. & Beach Thorofare

Ocean City, New Jersey 08226

TABLE OF CONTENTS

PAGE NUMBER

LIST OF FIGURES

I ABSTRACT

A program was undertaken to assess the severity of
fire retardant caused corrosion on air tankers and mixing plants.
A representative number of air tankers and mixing plants were
inspected and comprehensive laboratory tests were conducted to
identify and quantify the extent of different types of corrosion.
In the laboratory tests, five fire retardants and ten alloys were
investigated. The laboratory tests also included evaluation of
ten protective coatings for use as maintenance coatings and
evaluation of different chemicals for use as corrosion inhibitors
in retardant solutions. The results of the investigation are
presented with recommendations for control of fire retardant
corrosion.

II CONCLUSIONS

A. The aerial fire retardants currently used to suppress forest fires corrode aircraft and ground mixing equipment.

B. Corrosion of aircraft and ground mixing equipment continues to create maintenance problems.

C. The corrosivity of fire retardants is not consistent; corrosion rates vary for each alloy depending on the particular retardant formulation.

D. Phos-Chek XA, Fire-Trol 100 and Phos-Chek 259 are relatively non-corrosive to aluminum alloys ($\approx$.1 mpy by alternate immersion test).

E. Fire-Trol 931-L is only mildly corrosive to aluminum alloys. ($\approx$1 mpy by alternate immersion test).

F. Fire-Trol 931-D corrodes 2024-T3 aluminum, zinc and magnesium at significant rates (>5 mpy by total immersion test).

G. Fire-Trol 931-L corrodes zinc and magnesium at significant rates (>5 mpy by alternate immersion test).

H. In laboratory tests, Fire-Trol 100 corrodes brass and magnesium at significant rates (>3 mpy by alternate immer-

sion test). Field surveys also showed that Fire-Trol 100 corrodes steel significantly which is contrary to the results of laboratory tests.

I. Phos-Chek 259 corrodes brass and zinc at significant rates (>5 mpy by alternate immersion test).

J. Overall, Phos-Chek XA is the least corrosive of the fire retardants. It does not cause significant corrosion on any of the alloys commonly found on air tankers or in ground mixing plants.

K. Almost all alloys will corrode excessively in uninhibited diammonium phosphate (15.0% solution, by weight), uninhibited ammonium sulfate (15.0% solution, by weight), and uninhibited ammonium polyphosphate (8.3% solution, P_2O_5 equivalent by weight). These chemicals should never be used as fire retardants without effective corrosion inhibitor additives.

L. Alternate immersion conditons are significantly more corrosive to naval brass than total immersion conditions.

M. Stainless steel alloys are virtually immune to general corrosion caused by fire retardants.

N. Galvanic corrosion can occur at significant rates (≈ 3 mpy) even with the use of corrosion-inhibited retardants.

O.   The addition of corrosion inhibitors to retardant formulas
      can effectively reduce corrosion.

P.   Fire retardants without corrosion inhibitors are conducive
      to both stress corrosion and corrosion fatigue. The
      corrosion inhibited formulations currently in use do not
      completely eliminate susceptibility to stress corrosion.

Q.   The corrosivity of fire retardants can be significantly
      reduced by the use of additional inhibitors. Further work
      as follows is required to identify the most effective in-
      hibitors:

      1.   Inhibitor Duration Tests

      2.   Stress Corrosion Cracking Tests

      3.   Corrosion Rate Versus Inhibitor Concentration Tests

      4.   Corrosion Rate Versus Dilution Tests

      5.   Corrosion Fatigue Tests

      6.   Inhibitor Combination Tests

R.   Fire retardants rapidly deteriorate many of the common
      maintenance coatings. Certain epoxy-base coatings will
      provide adequate protection as maintenance coatings.

S.   The current interim USFS specification is realistic in
      limiting the maximum allowable corrosion rate to 1 mpy on

2024-T3 aluminum. However, the specification should be expanded to include other alloys and other types of corrosion test. Also, the test procedure should be modified to account for corrosion rate - time effects and differences that might occur under conditions of alternate immersion.

III RECOMMENDATIONS TO CONTROL FIRE RETARDANT CORROSION

A. Uninhibited fire retardants are quite corrosive to almost all alloys. Use only those retardant formulations containing effective corrosion inhibitor additives.

B. Pyro causes severe corrosion on almost all alloys (except stainless steels). Pyro should never be used as a fire retardant without corrosion inhibitor additives.

C. Most of the inhibited fire retardant now used across the country corrode aluminum alloys at an insignificant rate. However, other alloys commonly used on air tankers are susceptible to appreciable corrosion caused by exposure to fire retardant. Therefore, continuing preventive maintenance is required to control corrosion. Normal maintenance procedures as established by the Federal Aviation Administration (Advisory Circular No. 43-4 dated 5-15-73) should be followed.

D. Fire retardants are conducive to galvanic corrosion. Where possible, avoid the following galvanic couples:
    1. Aluminum alloys coupled to either copper-base alloys or stainless steel alloys.
    2. Carbon or low alloy steels coupled to either copper-base alloys or stainless steel alloys.

3. Galvanized steel coupled to aluminum, steel, copper or stainless steel alloys.

E. Fire retardants corrode mild steel alloys sufficient to cause seizing of threaded fasteners, hinges, etc. Where seizing is a problem, substitute an austenitic Type 304 stainless steel.

F. Fire-Trol 100 and Fire-Trol 931-L are severly corrosive to magnesium alloys. In general, avoid the use of magnesium alloys on air tankers. When magnesium alloys are present on air tankers, take particular care to prevent either of the above-mentioned retardants from contacting magnesium alloys for any appreciable time.

G. Fire-Trol 931-L is corrosive to galvanized steel. On air tankers, do not allow Fire-Trol 931-L to contact galvanized control cables for any appreciable period of time.

H. Vapors given off by some of the aerial fire retardants appear to be significantly corrosive. Avoid entrapment of fire retardant vapor in air tankers and storage tanks by providing proper ventilation.

I. Fire retardants rapidly degrade most organic maintenance coatings. In mixing plant service, use amine-cured epoxy

coatings for general exterior maintenance. For coating
the interior of steel storage tanks, use a high build
coal tar epoxy coating.

IV RECOMMENDATIONS FOR FOREST SERVICE ACTION

A. Initiate further studies in the following areas:

1. Corrosion Inhibitors

2. Vapor Zone Corrosion

3. Corrosivity Variation of Liquid Ammonium Polyphosphate

4. Corrosion Rate Versus Viscosity

B. Initiate steps to effectively transfer the technology developed in this program for implementation by air operators and retardant suppliers.

C. Consider the acquisition of more sophisticated instrumentation that would enable more accurate determination of corrosion rates by electrochemical polarization methods.

D. Revise and expand USFS interim specification 5100-00301 and 5100-00302A to reflect the technology developed in this program. Specific items include:

1. Expand the corrosion testing to include determination of general corrosion rates not only on 2024-T3 aluminum but also 7075-T6 aluminum, naval brass, 4130 steel and magnesium.

2. Determine corrosion rates under both total immersion conditions and alternate immersion conditions.

3. Conduct the total immersion tests over at least 30 days. Determine corrosion rates by polarization measurements on the 1st, 3rd, 7th, 14th and 30th day in test. In addition, weigh each test specimen prior to and after the test to allow determination of corrosion rate by weight loss.

4. Conduct the alternate immersion tests over 30 days. Determine general corrosion rates by weight loss measurements.

5. Substitute double cantilever beam (DCB) type specimens for the U-bend specimens now specified to check for susceptibility to stress corrosion cracking. Include 2024-T3 aluminum and 7075-T6 aluminum in the SCC tests. The test should be total immersion for 30 days.

E. Consider modifying existing specifications on fire retardants so that corrosion inhibitor additives can be specified for different retardant solutions instead of qualifying proprietary formulas.

V EXPERIMENTAL APPROACH

A.   Field Surveys

A representative number of air tankers and retardant mixing facilities were inspected to assess the extent and degree of fire retardant-caused corrosion. In total, 62 air tankers and 27 retardant mixing plants were inspected. Appendix I identifies each air tanker and mixing plant.

In addition to inspecting aircraft and retardant mixing facilities, the project team interviewed air tanker pilots, mixing plant foremen, and aircraft maintenance personnel who were familiar with typical corrosion-associated maintenance problems.

B.   Laboratory Testing

Based on the results of the field survey and a review of available literature, a laboratory program was designed to investigate fire retardant caused corrosion phenomena under closely controlled experimental conditions. The program sought to characterize the susceptibility of the common alloys used in air tankers and mixing plants to the different modes of corrosion (e.g. general corrosion, stress corrosion, corrosion fatigue, etc.) with respect to the fire retardants currently in use. The program was also designed to provide meaningful data necessary for proper assessment of corrosion observed during the field inspection trips.

Ten alloys and five fire retardants were selected for inclusion in the laboratory tests. Table I and II present the alloys and fire retardants. The alloys are representative of those most commonly found on air tankers and in mixing plants. The fire retardants represent those that are now used most widely throughout the country. All fire retardants used in the laboratory tests were obtained from production lots. None of the fire retardants were analyzed to determine exact composition.

The laboratory tests were separated into different phases designed to investigate particular modes of corrosion. The experimental techniques employed in each phase are described below:

1.   General Corrosion

Two types of test were conducted in this phase - total immersion (2 months) and alternate immersion (6 months). The ten alloys selected for testing were exposed in each of the five fire retardants. The alternate immersion cycle consisted of exposure to retardant for 8 hours and air exposure for 16 hours. In the alternate immersion test, the alloy specimens were spray washed with fresh tap water bi-weekly. Also, in the alternate immersion test, the retardant test solutions were replaced completely once a month with fresh retardant solutions.

For the total immersion tests, the alloy specimens consisted of rectangular 1" x 4" x 1/8" rolled sheet stock. A wire was mechanically attached at one end and the connection sealed with epoxy. The wire facilitated electrochemical polarization measurements. All specimens were exposed with an as-received surface finish. Prior to exposure, each specimen was degreased in acetone, rinsed in de-ionized water and hot air dried. The alloy specimens were suspended via the wire in each of the five retardant solutions.

For the alternate immersion tests, circular specimens 1/8" thick x 2" diameter were used. Each specimen had a 1/4" diameter hole drilled in the center. The ten alloys were rack assembled by running a teflon rod through the 1/4" diameter center hole and spacing each specimen 1-inch apart using teflon insulating spacers. In addition, 3/4" diameter teflon washers were sandwiched on each side of the alloy specimens. This was done to create a crevice condition. Figure 1 shows an assembled test rack.

As was done for the direct immersion tests, the alloy specimens were exposed with an as-received surface finish. Prior to exposure, all specimens were cleaned, solvent degreased, rinsed, and hot-air dried.

Data acquisition for this phase of the program included electrochemical potential and polarization measurements as well

as weight loss measurements. General corrosion rates were cal-
culated from both the polarization measurements and weight loss
measurements. Figure 2 shows the instrumentation set up for
making polarization measurements. Appendix II shows the calcu-
lations required to determine corrosion rates from polarization
measurements. The polarization technique for calculating cor-
rosion rates is invaluable because it enables rates to be determined
instantaneously in situ without disturbing the alloy specimen.
In this way, corrosion rates can be characterized as a function
of time over the test period. Weight loss measurements provide
only time averaged data and would require multiple specimens in
order to determine a valid corrosion rate vs. time relationship.

    2.   Localized Corrosion

    Besides determining general corrosion rates for the
different alloy specimens in each of the five fire retardants,
each alloy specimen upon completion of the exposure test was
inspected for typical forms of localized corrosion such as
pitting, intergranular corrosion, exfoliation, crevice corrosion,
and de-alloying. Where applicable, the specimens were examined
under a metallurgical microscope. Pit depth measurements were
made using the microscope.

    Potentiodynamic polarization curves were run on each
alloy in each retardant in an attempt to identify critical pit-
ting potentials. The purpose of these measurements was to es-

tablish quantitatively, if possible, the relative propensity of the different retardants to cause pitting corrosion.

3. Galvanic Corrosion

Potential and polarization data were also acquired to allow prediction of galvanic corrosion rates (corrosion caused by dissimilar metal contact) in each fire retardant. Based on polarization data, galvanic corrosion rates were estimated for each of possible galvanic couples that could occur between the 10 alloys under study. Appendix III describes these techniques.

4. Stress Corrosion

Two types of test specimens - U-Bend and DCB - were used to study the susceptibility of the ten alloys to stress corrosion when exposed to fire retardant. A typical U-Bend specimen is shown in Figure 3. The U-Bend specimens were prepared by deforming a flat coupon (1" x 4" x 1/16") around a cylindrical mandrel to form an open U shape. After forming, the U-Bends were stressed additionally to 75% of yield strength by inserting a bolt through two pre-drilled holes at the ends of the coupon and tightening the nut the required amount. The deflection on the U-Bend required to give a load equivalent to 75% of yield strength is calculated as follows:

$$y = (2\ \sigma\ l^2) \div (3\ E\ t)$$

where,   y = deflection of one arm of the U-Bend

σ = stress = fixed % of yield strength

l = gauge length of specimen = 1/2 (L-C/2)

E = Modulus of Elasticity

t = specimen thickness

L = specimen length

C = circumference of mandrel

The total deflection in a stressed U-Bend is 2y. After stressing the U-Bend specimens to the desired level, the specimens were cleaned, solvent degreased, rinsed and hot air dried. The bolted end of the U-Bend specimen was also masked with an epoxy coating to avoid galvanic effects. The U-Bend specimens were then totally immersed in each of the five fire retardants for a period of three months. The specimens were inspected weekly for evidence of cracking. The fire retardant test solutions were replenished monthly with fresh fire retardant.

In addition to U-Bend type specimens, pre-cracked double cantilever beam (DCB) specimens were also tested. This type of test specimen is generally more discriminating than the U-Bend specimen. The reason for this is that the time-to-failure data for U-Bend specimens includes both the initiation and propagation phases of stress corrosion cracking. Often, the crack initiation phase of the stress corrosion process is several orders of magni-

tude greater in time than the crack propagation phase. Therefore, for a smooth U-Bend specimen, cracking might not occur until a pit is produced that sufficiently intensifies the applied stress. In a real structure, surface flaws of some form are invariably present. If an alloy is susceptible to stress corrosion, failure will generally occur much more rapidly in the presence of pre-existing surface flaws.

The DCB specimen is designed to characterize stress corrosion susceptibility quickly and quantitatively by determining the propensity for subscritical crack growth to occur in the environment of interest. The specimen incorporates a pre-crack so that the crack initiation phase of the stress corrosion process is circumvented. There is no question as to whether cracking has occurred.

Stress intensity (as opposed to stress) at the pre-crack tip can be calculated by an equation derived from fracture mechanics if plane strain conditions exist. Recent developments in fracture mechanics indicate that stress intensity rather than stress, by itself, dictates whether a crack will propagate. The stress intensity depends not only on the nominal stress but on the size and geometry of a crack-type flaw. For example, the stress intensity at the crack tip of the DCB specimen as shown in Figure 4 is calculated as follows:

$$K_1 = \frac{vEh \ [3h(a + 6h)^2 + h^3]^{.5}}{4[(a + 6h)^3 + h^2 \ a]}$$

where, K_1 = stress intensity factor ksi (in)$^{.5}$

        v = total deflection of the two specimen arms at the load point, in.

        E = modulus of elasticity, ksi/in.

        h = 1/2 of the specimen height, in.

        a = crack length measured from load point (centerline of loading bolt), in.

For this program, the specimen height, 2h, and width, b, were 1 inch. The specimen length was about 5 inches.

At a sufficiently high value of stress intensity, normally designated K_{Ic}, unstable fast fracture will occur. The value of K_{Ic} is not related to stress corrosion behavior, but if a specimen subjected to a K value less than K_{Ic} undergoes slow crack growth in the presence of a corrosive environment, then K will increase until it reaches K_{Ic} and unstable fracture occurs. Slow stress corrosion crack growth does not occur at all values of K and the minimum initial value at which environmentally sensitive crack growth occurs is designated K_{Iscc}.

Stress corrosion tests were performed using the DCB specimen by turning the loading bolt sufficient to cause a crack at the end of a machined notch. For fixed displacement conditions at the bolt, K decreases rapidly as crack length increases. Thus, the initial pop-in crack runs only a very short distance before arresting. By measuring the crack

length and corresponding v value, a K_{Ic} value was calculated from the above equation.

Prior to exposing the DCB specimens, the bolt ends of the specimens were masked with an epoxy coating to avoid galvanic action effects. The specimens were then exposed in each fire retardant for a minimum duration of 1000 hours. The specimens were inspected for crack growth after 1, 10, 50, 100, 500, and 1000 hours. If an alloy is susceptible to stress corrosion cracking, crack growth should occur. The crack length at which growth ceases is then used to calculate K_{Iscc}.

For the stress corrosion phase of the program, two of the ten alloys (SAE 4130 steel and Type 410 Stainless Steel) were given special heat treatment. The stress corrosion behavior of these two alloys is particularly sensitive to prior heat treatment history. Both alloys were heat treated to hardness levels which have shown extreme stress corrosion susceptibility in other environments. It was thought that if both of these steels proved to be unaffected in their most susceptible heat treatment condition, then it could be safely concluded that the fire retardants would not cause stress corrosion.

The SAE 4130 Steel was heat treated to a Rockwell C hardness of about 40 (UTS $\approx$ 186 ksi) as follows:

1550°F, 1/2 hour in salt, oil quenched

plus,

800°F, 2 hours in air, air-cooled

SAE 4130 steel with this heat treatment is much harder and more brittle than the 4130 grade of steel normally used in aircraft structures. The more ductile grade of 4130 steel used in aircraft is more resistant to stress corrosion.

The type 410 stainless steel was heat treated to an R_c hardness of about 38 (UTS $\simeq$ 180 ksi) as follows:

1832°F, 1/2 hour in salt, oil quenched

plus,

1000°F, 2 hours in salt, air-cooled

Again, type 410 stainless steel heat treated in this fashion is atypical of the stainless steels commonly used in air tankers.

For aluminum alloy sheet, the grain structure usually exhibits a preferred orientation (longitudinal, long transverse, or short transverse) relative to the rolling direction. Susceptibility to stress corrosion usually varies dependent on the direction of applied load relative to grain orientation. The short transverse orientation is generally the most favorable for crack propagation while the longitudinal orientation is the least favorable. For these tests, the U-Bend specimens were stressed

along the longitudinal axis, the least susceptible orientation. The DCB specimens were stressed parallel to the short transverse axis, the most susceptible orientation.

5.   Corrosion Fatigue

This phase of laboratory testing investigated three of the ten alloys considered most susceptible to corrosion fatigue. The alloys included in the testing were:

1.   2024-T3 Aluminum
2.   7075-T6 Aluminum
3.   SAE 4130 Steel

The 2024 alloy is commonly used as an aircraft "skin" alloy while the 7075 aluminum and 4130 steel are used widely for aircraft structural members such as spars, wheel treadles, etc. The susceptibility of each of these alloys to corrosion fatigue in the five fire retardants was investigated by subjecting 1/2" x 1/4" x 14" notched test specimens of each alloy to cyclic loads while exposed to the retardants. Figure 5 shows the typical test set up.

Initially, fatigue curves were determined for each of the three alloys in air. Subsequently, fatigue data was acquired in each fire retardant. The tests were conducted on single-edge

notched cantilever beam specimens using a Vishay VSP-150 plate bending machine. The cyclic test frequency was 100 cpm for all tests. Sinusoidal stress waves of varying amplitudes were applied and the cycles-to-failure recorded. Test runs were conducted thru 10^6 cycles. The fatigue data gathered in each of the fire retardants were compared with the data gathered in air. If the fire retardants created conditions favorable for corrosion fatigue, it was expected that the alloy test specimens would exhibit lower cycles-to-failure in fire retardant when subjected to the same cyclic load.

The cyclic load was applied parallel to the long transverse grain orientation of the aluminum alloys. Aluminum alloys are known to exhibit different fatigue behavior dependent on the relationship of applied stress to grain orientation. The short transverse direction is the most susceptible while the longitudinal direction is the least susceptible. Testing in the short transverse direction would have added significant cost to the program and was considered to be beyond the scope of work required at this time.

6.   Corrosion Inhibitor Evaluation

This phase of the laboratory test program was intended to identify and evaluate different chemicals that might qualify as effective corrosion inhibitors when added to fire retardants.

First, a literature search was conducted to determine ten (10) candidate corrosion inhibitors. Upon completion of the literature search, short term screening tests were initiated to quantitatively rate the candidate inhibitors. Based on the results of the short term screening tests, three (3) inhibitors were selected for further evaluation. This further evaluation included 30-day total immersion tests, stress corrosion tests using DCB specimens, and corrosion fatigue tests.

The short term screening tests were conducted using three (3) base retardant solutions. The three solutions were as follows:

       a.   Diammonium Phosphate (15%, by weight)

       b.   Ammonium Sulphate (15%, by weight)

       c.   Ammonium Polyphosphate (10-34-0, 4:1 dilution)

These three solutions essentially comprise the bulk of the chemicals now used for aerial fire retardants. Depending on manufacturer, thickening agents, spoilage inhibitors, and corrosion inhibitors are added in varying degrees to one of these solutions. From a corrosion standpoint, it was assumed that the base retardant solutions would have the major effect on corrosion whereas the effect of the thickening agents and spoilage inhibitors would be minimal. Of course, the corrosion inhibitors used in proprietary formulas had to be eliminated in order to meaningfully evaluate each individual inhibitor selected for testing.

Each of the ten candidate inhibitors was added at 1%
by weight, to each of the three base solutions. The ten alloys
tested in previous phases of the program were then immersed in
each solution for 24 hours. After 24 hours in solution, general
corrosion rates were determined for each alloy in each solution
by polarization measurements. The relative effectiveness of
each of the ten inhibitors was rated from this data.

From these short term tests, the three best inhibitors
were further evaluated by extending the exposure period from
24 hours to 30 days. General corrosion rates were measured by
polarization measurements at periodic intervals and also
determined by weight loss measurements at the end of the tests.
The effects of each of the three inhibitors on galvanic corrosion
and stress corrosion were also characterized using test methods
similar to those previously described. This testing was limited
to the worst cases predicted from previous tests. In addition,
one of the inhibitors was evaluated as to its relative effect
on corrosion fatigue using test methods already described.

7.   Protective Coating Evaluation

The field inspection trips indicated that many of the
maintenance coatings in use at various mixing plants were
providing less than adequate service. Therefore, this phase
of the laboratory program concentrated on identifying and

evaluating protective coatings applicable under conditions normally encountered in the field that might provide improved service in the subject environment.

A literature search was conducted to define candidate coatings for testing and evaluation. The most important criteria for selection were: apparent stability in an environment similar to that of a fire retardant mixing plant; insensitivity to adverse application conditions; good abrasion and impact resistance; good appearance; and relative cost.

Insensitivity to adverse application conditions was considered an important criteria because the coatings are almost always applied on site. It is, therefore, usually impractical or impossible to provide a sandblasted surface. Also, climatic conditions such as temperature and humidity are often less than ideal for coating application. Abrasion and impact resistance are important because of the type of activity characteristic of mixing plant operation.

Based on the results of the literature search, eleven (11) coatings were selected for testing. Each of the coatings was applied according to manufacturer's recommended procedures to three 3" x 6" x 1/4" hot rolled steel panels. The surfaces of the steel panels were pre-rusted by exposing them, after degreasing to a periodic salt water spray until the surfaces were sufficiently

rusted. All loose rust was then removed by wire brushing. This surface condition simulates the typical surface condition found in the field.

All of the coated test panels were then partially immersed (about 75% of the panel area) in each of the base retardant solutions used in the inhibitor evaluation phase already described. The duration of exposure was three months. The relative performance of each of the coatings was quantitatively rated by periodic electrical impedance measurements. The coated panels were also visually inspected at periodic intervals for obvious deterioration. At the end of the test period, the coatings were ranked on their relative resistance to a fire retardant environment.

VI DISCUSSION OF RESULTS

A. Field Surveys

The first thing that became obvious in discussions
with people associated with air tanker operations was the wide
difference in opinion on the corrosivity of aerial fire
retardants. There are strong feelings as to the relative
corrosivity of the different retardants now in use. Many of
these feelings are justified, many are not. Hopefully, this
discussion will help to clear up much of the misconception
regarding the corrosivity of aerial fire retardants by offering
meaningful quantitative evidence to support all conclusions.

Inspection of aircraft and retardant mixing equipment
during field surveys showed obvious corrosion on hardware compo-
nents. In most instances, it was difficult to immediately
assess the principal cause of the observed corrosion because
the aircraft or mixing equipment had been exposed to a variety
of fire retardants some of which are no longer in use. Another
factor is that some of the aircraft were used in other types
of service such as crop spraying. However, in conjunction
with the results of the subsequent laboratory tests, reasonable
assessment can be made of field observations.

Appendix IV presents a list of the different types of corrosion observed during the course of the field inspection trips. Figures 6 thru 16 show some of the typical corrosion damage. In general, corrosion of aluminum alloy components appears to have been greatly reduced by the development of the retardant formulas which contain effective corrosion inhibitors. Inspection of aircraft and mixing equipment exposed only to these retardants usually showed minimal corrosion of aluminum hardware. The laboratory tests tend to confirm this and indicate that the general corrosion rate for most aluminum alloys exposed to Phos-Chek XA, Fire-Trol 100, and Fire-Trol 931-L should fall somewhere between .1 and 1 mpy. In cases where significant corrosion of aluminum components was observed, the aircraft had usually been exposed to another retardant (Algin Gel, uninhibited DAP, uninhibited Pyro, etc.).

There were isolated instances where significant pitting of aluminum did occur on hardware that had been exposed to Phos-Chek XA, Fire-Trol 100 and/or Fire-Trol 931. There is no conclusive evidence at this time as to why such attack occurred. These isolated cases might be the result of poor quality control. Also, corrosion caused by entrapped retardant vapor might have been contributory. Vapor zone corrosion was not investigated in the laboratory phase of this program.

The laboratory tests (alternate immersion) did indicate that Phos-Chek XA and Fire-Trol 100 should corrode aluminum

alloys at approximately .1 mpy. Fire-Trol 931-L (LC) appears slightly more corrosive causing aluminum alloys to corrode between .5 and 1.3 mpy. For comparison, uninhibited LC tends to corrode aluminum alloys at about 5 mpy - which is roughly the rate unprotected steel corrodes in sea water. None of these corrosion rates are excessive and it would appear that aluminum alloys can be safely used on aircraft without a protective coating.

Although the three major retardant formulas currently in use are relatively non-corrosive to aluminum alloys, some other alloys do not fair as well. Copper-base alloys corrode at significant rates in Fire-Trol 100. There were a number of instances during the inspection trips where significant corrosion of copper-base alloys was observed. This corrosion seemed to correlate with exposure to Fire-Trol 100. Laboratory tests showed that under an alternate immersion cycle, naval brass in Fire-Trol 100 corrodes at about 4 mpy. The corrosion rate in the total immersion test was significantly lower ($\simeq$ .1 mpy). The alternate immersion test is considered more typical of the actual environment. Fire-Trol 100 also tends to give off ammonia vapor which accelerates corrosion of copper-base alloys.

Severely corroded magnesium alloy components (wheel rims, hydraulic cylinder caps) were also seen during the field inspection of aircraft. Figure 17 shows the deep pitting corrosion

that occurred on a hydraulic cylinder cap. Laboratory data indicates that Fire-Trol 100 and Fire-Trol 931 L&D corrode magnesium alloys at rates exceeding 100 mpy. Phos-Chek XA is appreciably less corrosive ($\simeq$ 1 mpy).

Corrosion was detected on various steel components throughout the inspection trips. Corrosion rates established in the laboratory for the three major retardants ranged from about .5 to 1 mpy. While steel corroding at this rate is not considered excessive, it is sufficient to cause seizing problems. This problem was observed most often on tank gate adjustment mechanisms where threaded fasteners had been used. Also, steel torque tubes in the gate opening mechanism tend to freeze.

The worst corrosion of steel detected during the field survey was corrosion above the air-retardant interface in steel tanks storing Fire-Trol 100. The general corrosion rate was estimated to be about 25 mpy. The same degree of attack was not observed in the total immersion or alternate immersion tests conducted in the laboratory. The alternate immersion tests did show a higher corrosion rate (1.2 mpy vs. .5 mpy) than the direct immersion tests for steel exposed in Fire-Trol 100. The accelerated corrosion of the steel might have been caused by entrapped vapors given off from the Fire-Trol 100. Further work is required to confirm this.

While no significant corrosion was detected on zinc alloys or galvanized steel during the field inspection, laboratory tests show that Fire-Trol 931 D&L are quite corrosive to zinc (initial corrosion rates exceeded 100 mpy as shown in Table IV).

Galvanic corrosion between aluminum and steel in retardant tanks on aircraft was detected on several occasions. Laboratory measurements indicate that corrosion will occur on aluminum when coupled to steel at rates approaching 2.5 mpy when exposed in Fire-Trol 931 and Phos-Chek XA on an equal area basis. In Fire-Trol 100, laboratory measurements indicate that aluminum is actually noble to steel in some instances (2024 Al, 2024 Alclad) and therefore corrosion of the steel would tend to accelerate when coupled to aluminum.

During the field survey, there was little evidence of fractured components that might be related to stress corrosion or corrosion fatigue phenomena. A B-17 (C-19, N5230 V) did suffer a cracked 4130 steel wing spar. A subsequent metallurgical report prepared by another laboratory established that the spar had evidently been heat treated improperly resulting in a loss of ductility. Ultimately, a fatigue crack initiated. It seems remote that this particular crack was accelerated by fire retardant caused corrosion. Laboratory tests showed, however, that uninhibited ammonium polyphosphate can cause corrosion fatigue.

Popping of stainless steel bolt heads occurred in the retardant tanks of another aircraft. The exact cause of these bolt failures could not be determined. The bolts were made from a Type 431 martensitic grade stainless steel. It is possible that the failures were simply the result of mechanical overload or were caused by stress corrosion. It is also possible that galvanic current flow between the aluminum tank and stainless steel bolt caused hydrogen absorption on the stainless steel and subsequent hydrogen embrittlement. Laboratory tests showed that martensitic stainless steels are susceptible to stress corrosion in uninhibited ammonium polyphosphate. Laboratory tests also showed that high strength SAE 4130 steel (similar in behavior to Type 431 stainless) is susceptible to stress corrosion in all of the fire retardants. Austenitic Type 304 stainless steel in an annealed condition resisted stress corrosion. Type 304 stainless steel would seem to be a better choice for fastener alloy since it is generally more resistant to stress corrosion cracking and hydrogen embrittlement than the martensitic stainless steel.

The field inspection trips showed that the most significant deterioration of protective coatings is occurring in retardant mixing plants. Almost all types of common organic maintenance coatings are now being used. In a majority of cases, the protective coatings are not providing adequate service.

The laboratory tests confirmed that aerial fire retardants will rapidly degrade many of the organic maintenance coatings. Out of eleven different generic types of coatings tested, only two epoxy-base coatings provided acceptable service in all base retardant solutions.

One aspect of fire retardant caused corrosion that was not investigated in the laboratory but appears to be occurring in isolated instances is corrosion due to retardant vapor. Vapor zone corrosion seems to occur in areas where vapors tend to become entrapped. Fire-Trol 100 seems especially conducive to vapor zone corrosion. This phenomena should be further investigated.

None of the aircraft or mixing equipment which were inspected had been exposed to uninhibited ammonium polyphosphate (Pyro) for an appreciable period of time nor to Phos-Chek 259 which is used for ground application. Both of these fire retardants were included in the laboratory test program. No correlation of the effects of these two retardants can be made based on the field surveys. However, the liquid ammonium poly-phosphate solution is essentially the base solution for Fire-Trol 931 without inhibitors. The laboratory tests showed that unin-hibited ammonium polyphosphate is quite corrosive to most alloys. This points out the importance and necessity of effective inhibitor treatment to control corrosion.

B.   Laboratory Tests

Different phases of the laboratory test program were briefly mentioned in discussing and assessing what had been observed on field inspection trips. The following presents a detailed discussion of the laboratory results:

1.   General Corrosion

Table III presents the general corrosion rates for both the total immersion exposure test and alternate immersion exposure test determined from weight loss measurements. Table IV presents general corrosion rates determined by polarization measurements at different time intervals over the 2 month total immersion test period. Table V compares the general corrosion rates calculated from polarization measurements with the corrosion rates determined by weight loss for the total immersion tests. Figures 18 thru 22 show this same data in bar graph form to demonstrate the excellent agreement between the two methods used to determine corrosion rates. Table VI presents the average electrochemical potential measurement for each alloy in each retardant over the 2-month total immersion tests.

The data shows that the stainless steel alloys are virtually immune to general corrosion in fire retardant. The magnesium alloy corroded rapidly in the Fire-Trol formulations and in Pyro but exhibited a comparatively low corrosion rate in the Phos-Chek

formulations. Zinc corroded rapidly in Pyro and Fire-Trol
931 but exhibited significantly lower corrosion rates in Fire-
Trol 100 and the Phos-Chek formulations.

The weight loss data do not give a true indication of
the corrosion rate for zinc because of the form in which zinc
was tested. Zinc was tested as a hot-dip galvanized coating on
SAE 1010 steel. The coating thickness was approximately 5 mils.
Polarization measurements show that zinc corrodes initially in
Pyro and Fire-Trol 931 at a rate exceeding 100 mpy. Consequently,
in these solutions, most of the zinc coating is removed within a
few days. In effect, the remainder of the test period consisted
of an exposure test on SAE 1010 steel. In Pyro, steel also cor-
rodes at an extremely high rate whereas in Fire-Trol 931, steel
corrodes at a low rate. Therefore, the difference in corrosion
rate observed in the alternate immersion test for zinc in these
two solutions can be attributed more to the difference in be-
havior of 1010 steel than zinc.

The electrochemical potential measurements also proved
helpful in identifying this phenomena. The initial potential for
zinc in both solutions was approximately -1.05 volts to a Ag/AgCl
reference electrode. Over the first few days in test, the poten-
tial dropped off sharply to about -.700 volt. This potential is
more characteristic of steel than zinc. In the other retardants,
the potential for zinc averaged around -.900 volts over the entire
test period.

In the total immersion test, the 2024-T3 aluminum alloy exhibited a high corrosion rate ($\approx$ 7 mpy) in Fire-Trol 931. However, in the longer term alternate immersion test, the corrosion rate for the same alloy was 1.3 mpy. This corrosion rate is slightly higher than that permitted by current USFS specifications.

The corrosion of the other aluminum and steel alloys was not excessive except in Pyro. For the aluminum alloys, the alternate immersion test seemed to be less corrosive than the total immersion test. The exception was Fire-Trol 100 where the total immersion condition was less corrosive. For the steel alloys, the alternate immersion test proved worse in three retardants while the total immersion test was worse for the other two. The alternate immersion test is thought to be more representative of service conditions.

For naval brass, the alternate immersion test produced a very significant increase in corrosion rate over the total immersion test. In every case except one, there was at least an order of magnitude increase in corrosion rate. Brass corroded at significant rates in Fire-Trol 100, Phos-Chek 259, and Pyro under alternate immersion conditions.

2.   Localized Corrosion

a.   Crevice Corrosion - There was almost no evidence of crevice corrosion on the test specimens exposed

in the exposure tests. This was surprising since the aluminum and stainless steel alloys are notoriously susceptible to crevice corrosion. The absence of crevice corrosion in the fire retardant solutions might be associated with the lack of chlorides. The presence of chlorides is known to greatly accelerate crevice corrosion.

b.   Pitting Corrosion - In general, the aluminum alloys exhibited general light etching as opposed to localized pitting. The only aluminum alloy which exhibited pitting was the 6061-T6 alloy in Pyro. The average pit depth was about 1.4 mils.

As with the aluminum alloys, most of the other alloys exhibited general surface etching rather than localized attack. There was no visible attack on the stainless steels.

The potentiodynamic polarization scans did not distinguish clear-cut pitting or breakdown potentials for any alloy. This is not surprising in view of the general absence of localized pitting.

c.   Intergranular Corrosion - The only evidence of intergranular corrosion appeared to occur on 7075-T6 aluminum in Pyro.

d.   De-alloying - Shallow dezincification was evident on the brass alloy exposed to Phos-Chek 259.

e. Exfoliation - None of the aluminum alloys showed exfoliation at the end of the expousre tests.

3. Galvanic Corrosion

Table VII presents the five worst cases of galvanic corrosion predicted for each of the five retardants from electrochemical potential and polarization data. The rates have been calculated assuming equal areas for each of the alloys in the couple. In service, area ratios are not usually equal. The data does provide an insight as to what effect the retardants might have on galvanic corrosion.

In Fire-Trol 100, some of the aluminum alloys are more noble than steel by at least 60 millivolts. Thus, steel would corrode in preference to aluminum. Usually, in galvanic couples involving aluminum and steel, aluminum corrodes. In Phos-Chek XA, for example, 2024 aluminum coupled to 4130 steel would galvanically corrode at about 1 mpy. The galvanic corrosion rate is additive with the general corrosion rate. Therefore, 2024 aluminum might exhibit a total corrosion rate approaching 2.5 mpy assuming a general corrosion rate of 1.5 mpy as determined in the total immersion tests. The total corrosion rate for the same couple in Fire-Trol 931 is also about 2.5 mpy while in Pyro, the total corrosion rate approaches 13 mpy (galvanic rate $\simeq$ 3 mpy, general rate $\simeq$ 10 mpy).

The practical implications of this data are obvious. If the tank and gates on an air tanker were fabricated from 2024 aluminum with a 4130 steel torque tube, the torque tube would galvanically corrode when exposed to Fire-Trol 100. However, if the air tanker carried Phos-Chek XA, the aluminum tanks would galvanically corrode.

The importance of both potential and polarization behavior in influencing galvanic corrosion can be seen if one considers the 7075 aluminum - 4130 steel couple in Fire-Trol 931 and in Pyro. In Fire-Trol 931, the potential difference between the two alloys is 130 millivolts. In Pyro, the potential difference is only 30 millivolts. One might expect, therefore, that Fire-Trol 931 would be worse on galvanic corrosion. However, if one examines the polarization behavior of both alloys in each retardant, it is evident that exposure in Pyro will be the worst case. Figures 23 and 24 show the polarization curves for each couple and the calculation of the galvanic corrosion rate.

The data indicates that galvanized steel will corrode rapidly if galvanically coupled to any of the other alloys. The data on galvanized steel was omitted for Fire-Trol 931 and Pyro in Table VII because the zinc coating corrodes rapidly even in the absence of a galvanic couple. The magnesium alloy was omitted from consideration in this phase of the program since it corrodes rapidly, by itself, in almost all retardants.

Because of the low electrical resistivity of the fire retardants, (10 to 20 ohm-cm), it was thought that the galvanic corrosion rates would be appreciably greater than indicated by the electrochemical data. "IR" polarization effects are usually inconsequential in low resistivity solutions and galvanic corrosion rates tend to be high. However, the inhibitors added to the fire retardants are evidently limiting the galvanic corrosion process by controlling polarization behavior.

4. Stress Corrosion

No cracking was detected over a 3 month period on any of the U-Bend specimens. The magnesium alloy was not tested because it could not be deformed into an open U shape without fracturing the test specimen. Table VIII presents tensile strength data for each of the alloy specimens.

The DCB tests did show that certain alloys are susceptible to stress corrosion cracking in different fire retardants. Table IX lists the alloys and retardants where environment caused crack growth occurred as well as the calcualted values for K_{Ic} and K_{Iscc}. K_{Ic} and K_{Iscc} values were calculated only for the aluminum alloys and 4130 steel alloy. K_{Ic} and K_{Iscc} calculations are not valid for the brass alloy because plane strain conditions did not exist (the alloy is very ductile).

The 410 stainless steel alloy was tested only in Pyro. All of the other 410 stainless steel DCB specimens cracked through to the sides during pop-in of the initial crack. The 410 alloy was heat treated to a high hardness, brittle condition and, as such, is not readily adaptable for testing using DCB techniques. The DCB specimen of 410 stainless steel that was tested in Pyro did show crack growth. However, valid K_{Iscc} calculations could not be made because crack branching occurred (Figure 25). Figures 28 thru 30 show some of the test specimens after exposure.

For the aluminum alloys, Table IX shows that the 6061 and 7075 alloys are susceptible to stress corrosion cracking in the Phos-Chek formulations. The 2024 aluminum alloy is susceptible in Fire-Trol 931 and Pyro. The only cases where there was a significant reduction in stress intensity required for cracking were 6061 aluminum in Phos-Chek XA and 7075 aluminum in Phos-Chek 259. The rest showed only a minimal reduction in threshold stress intensity. The naval brass alloy exhibited cracking in three retardants - Phos-Chek XA, Fire-Trol 100 and Pyro. The 4130 steel alloy showed significant crack growth in every retardant. In some cases, there was a net reduction of over 50% in stress intensity required for cracking. Figures 26 and 27 show typical test specimens.

The DCB tests as conducted have shown that each fire retardant under the right conditions can cause stress corrosion

cracking. However, from a practical standpoint, the problem
might not be as serious as it first appears. The major alloys
of concern are 7075 Al, 2024 Al and 4130 steel because these
are the prime structural alloys used on air tankers. The only
case where 7075 aluminum showed a significant decrease in
threshold stress intensity was in Phos-Chek 259. This retardant
is not normally carried by air tankers. In all other cases, the
7075 and 2024 alloys showed only a minimal reduction in threshold
stress intensity.

The 4130 steel alloy was tested in a high strength,
high hardness condition where it is most susceptible to stress
corrosion. In aircraft structures, 4130 steel is usually speci-
fied in a lower strength condition. In the lower strength con-
dition, 4130 steel is much less susceptible to stress corrosion.

The fact that the tests have demonstrated stress cor-
rosion susceptibility does point out the need for continuing
conscientious maintenance of air tankers. Maintenance of the
air tankers should include periodic inspection for cracking
of structural members. Also, the aircraft should be washed
off frequently to avoid prolonged contact of the fire retard-
ant with critical structural members.

5.   Corrosion Fatigue

Figures 28, 29, and 30 present fatigue data obtained
in each of the fire retardants for 2024-T3 aluminum, 7075-T6

aluminum and SAE 4130 steel.

The tests conducted on the 2024-T3 aluminum suggest that in the long transverse grain orientation, the only fire retardant which increases the susceptibility to fatigue failure is Pyro. This is obvious from Figure 28. Three different test specimens were cyclically loaded at 8,500 psi while exposed to Pyro. Fatigue failure occurred at 1.85×10^5, 3.80×10^5, and 3.89×10^5 cycles. Fatigue failure on the specimens exposed to air occurred at 6.61×10^5, 7.81×10^5, and 1.108×10^6 cycles. It is apparent that exposure to the Pyro decreased the effective lifetime of the aluminum alloy under cyclic loading.

The other four fire retardants included in the tests extended the effective lifetime of the 2024-T3 aluminum beyond that determined in air. This effect is probably related to the presence of the different inhibitors in these fire retardants. The inhibitors might tend to prolong the time required for crack initiation. It appears that none of the four retardants will accelerate fatigue crack growth in the long transverse direction of rolled 2024-T3 aluminum plate.

The fatigue data for 7075-T6 aluminum does not show a significant difference in cycles-to-failure for Pyro versus cycles-to-failure in air. Again, the data suggests that the other four retardants tend to extend the cyclic fatigue life beyond that determined for air.

For 7075-T6 aluminum, branching of the fatigue crack sometimes occurred on test specimens exposed in fire retardant (Figure 31). When this occurred, the mode of crack propagation changed from transgranular in the long transverse direction to intergranular in the short transverse direction. The branched cracks would ultimately arrest. Failure would then occur at the maximum load point on the test specimen not exposed to the fire retardant.

Apparently, the fire retardant makes crack propagation in the short transverse direction energetically more favorable. However, once the direction of cracking changes to the short transverse orientation, it is parallel to the direction of applied stress. Propagation of the crack then arrests. The occurrence of this phenomena might distort the fatigue data. Although the fatigue data suggests that fire retardants will not accelerate cracking when the aluminum alloy is stressed parallel to the long transverse grain orientation; it may be that there is a significant reduction in resistance to fatigue when the alloy is cyclically stressed in the direction parallel to the short transverse orientation. Fatigue testing in the short transverse grain orientation was beyond the scope of the present program.

The fatigue data for 4130 steel is similar to that for 2024 aluminum in that the only fire retardant which tends to increase corrosion fatigue susceptibility is Pyro. At a

cyclic load of 33,000 psi, fatigue failure occurred in Pyro @ ≃ 25,000 cycles and in air @ ≃ 180,000 cycles. At a cyclic load of 26,500 psi, fatigue failure occurred in Pyro @ 34,000 cycles and in air @ ≃ 130,000 to 500,000 cycles. The other four retardants did not significantly reduce the endurance limit of 4130 steel from that obtained in air.

It should be noted that the effects of the fire retardants on fatigue life are only evident at the lower stresses where the fatigue lifetimes are greater. At the lower fatigue lifetimes (≃ 10^3 cycles), time dependent corrosion phenomena do not have enough time to react with the material. For example, a 10^3 cycle run-out @ 100 cpm is equivalent to about 10 minutes whereas a 10^6 cycle run-out @ 100 cpm is about 7 days. Therefore, fatigue data in fire retardants at the higher stress levels were omitted.

6. Corrosion Inhibitor Evaluation

    a. Literature Search - Table X lists the chemicals selected as candidate inhibitors for study in this phase of the program. The selection was based on a thorough review of available literature. All of the inhibitors are non-proprietary chemical compounds and are commercially available.

Sodium mercaptobenzothiazole is a widely known and used inhibitor for aluminum, steel and copper alloys. It is

-45-

primarily used in antifreezes and petroleum products but has also been found effective in chemicals including fertilizers.

Sodium dichromate is another inhibitor widely used to control corrosion of aluminum, copper, magnesium and zinc alloys in salt solutions. Some success has been reported with the use of sodium dichromate in ammonium phosphate fertilizers as an inhibitor.

Sodium fluorosilicate is a useful inhibitor for aluminum alloys. Brass, copper, lead and zinc alloys are also protected by the use of silicate inhibitors.

Sodium ferrocyanide is reported in the literature as being effective for controlling corrosion of cooling tower facilities. Alloys protected include aluminum, brass and iron.

Thiourea has diverse applications as an inhibitor in the chemical industry. It has been investigated as an inhibitor for use in fertilizers as well as in solutions containing chloride and sulfate ions. Both iron and aluminum alloys are listed in the literature as being protected by thiourea.

The literature search defined ammonium fluoride as being effective in mono - and diammonium phosphate fertilizer solutions.

Sodium nitrite is a useful chemical for inhibiting corrosion in salt solutions. Both aluminum and steel alloys are protected by sodium nitrite.

Amines can be used to protect aluminum from corrosion. Dimethylamine has been shown in the literature to be effective against corrosion of aluminum in chloride solutions.

Aniline sulfate is listed in the literature as being effective in the corrosion control of aluminum. It has been primarily tested in antifreeze solutions.

According to the literature, ammonium thiocyanate is effective in controlling corrosion of aluminum alloys in fertilizers. Copper is also reported as being protected in solutions containing sulphate ions.

     b.   Short Term Screening Tests - Tables XI, XII, and XIII present the results of the short term screening tests in each of the three base retardant solutions. From Table XI, sodium dichromate appears overall to be the most effective inhibitor in 15% diammonium phosphate. Ammonium fluoride also appears overall to be a worthwhile inhibitor. Sodium mercapto-benzothiazole is effective on the steel, brass, zinc and magnesium alloys, but has little beneficial effect on the aluminum

alloys. Except for 2024 Alclad, the sodium fluorosilicate inhibitor is beneficial for the aluminum alloys. Sodium dichromate was selected for the long term tests since it was the best overall.

In 15% ammonium sulfate, almost all of the inhibitors tested reduced the corrosion rate on aluminum alloys to reasonable levels. Table XII presents the results. Sodium ferrocyanide, aniline sulfate, sodium mercaptobenzothiazole, ammonium thiocyanate, and dimethylamine produced very low corrosion rates on the aluminum alloys. Sodium ferrocyanide was selected for the long term tests because it exhibited the best results on aluminum alloys and also produced good results on the other alloys.

In ammonium polyphosphate (10-34-0, 4:1 dilution), ammonium thiocyanate, sodium dichromate, and sodium MBT were the best inhibitors for the aluminum alloys. Overall, ammonium thiocyanate seemed to be the best candidate for further testing. Table XIII summarizes the results.

It was noted during the screening tests, that sodium ferrocyanide in polyphosphate formed a rather durable blue surface film on the test coupons. Sodium MBT formed an insoluble colloidal suspension in all solutions. Sodium fluorosilicate caused a gelatinous precepitate in diammonium phosphate.

c. Long Term Tests on Three Best Inhibitors - Table XIV presents the general corrosion rates determined for

the three best inhibitors over a 30-day test period. Each of
the inhibitors provided effective protection for the aluminum
alloys over the entire period. The corrosion rates determined
by polarization measurements at periodic intervals demonstrate
the time dependence of the corrosion process. For most alloys,
the corrosion rates decreased as a function of time. In general,
corrosion rates determined by polarization measurements agree
quite favorably with those determined by weight loss.

In addition to determining general corrosion rates for
each of the three inhibitors, the effect of the inhibitors on
galvanic corrosion was briefly investigated. Galvanic corrosion
rates were estimated for some of the couples that exhibited sig-
nificant corrosion rates in the galvanic corrosion phase of the
laboratory program. Table XV shows the results. In all cases,
the galvanic corrosion rates are minimal.

Each of the three inhibitors were also screened for
their ability to reduce stress corrosion cracking. Some of the
alloys and retardant solutions where stress corrosion suscep-
tibility had been detected in the earlier phase were investigated.
DCB type specimens were used. Table XVI presents these results.
As is evident, none of the inhibitors prevented crack growth.

Lastly, the ability of ammonium thiocyanate to reduce
corrosion fatigue susceptibility in Pyro was examined. It was

shown previously that Pyro increased susceptibility to corrosion fatigue. For 2024 Al, the thiocyanate inhibitor had no effect. In uninhibited Pyro, the average fatigue lifetime at a load of 12,000 psi was 333,000 cycles. With the thiocyanate inhibitor added, under the same load, cycles-to-failure were 341,500.

For 4130 steel, there was also no apparent beneficial effect. In uninhibited Pyro, at 26,500 psi, the cyclic lifetime was 34,000 cycles. With the thiocynate added, the cyclic life-time under the same load was 30,200 cycles.

The three inhibitors studied in this phase did ef-fectively reduce general corrosion and galvanic corrosion. The inhibitors did not, however, eliminate susceptibility to stress corrosion cracking, nor was the ammonium thiocy-anate inhibitor able to improve resistance to corrosion fatigue in Pyro.

The inhibitor evaluation phase of the program un-covered several inhibitors that would seemingly be effective in reducing fire retardant caused corrosion. Because of program limitations, only three inhibitors could be investi-gated in an in-depth manner. Seven out of the ten inhibitors tested appear to offer potential advantages in controlling fire retardant corrosion. To determine the most effective inhibitors and properly specify inhibitor additives for fire

retardants, additional tests beyond the scope of the present program are required. Additional testing should include the following:

a.   Inhibitor Duration Tests - Many chemicals possess corrosion inhibiting properties however often these properties are short term in nature. The duration over which a chemical is effective depends on the rate at which the inhibiting element is depleted due to the inhibition reaction or some other phenomena which tends to change or break down the inhibitor properties with time.

b.   Stress Corrosion Cracking Studies - These tests would rate the relative effectiveness of each candidate inhibitor in reducing stress corrosion cracking susceptibility. DCB-type specimens would be exposed in each inhibitor/retardant combination. These tests are more discriminating than U-Bend type tests as shown in the present program.

c.   Corrosion Rate Versus Inhibitor Concentration Studies - In the present program, all inhibitors have been arbitrarily screened at a concentration of 1%, by weight. It may be that significant advantages can be gained by either reducing or increasing the concentration of the various candidate inhibitors. Once the optimum concentration is determined for controlling corrosion, relative costs can be compared.

d.   Corrosion Rate Versus Dilution Studies - Aircraft metals are commonly exposed to diluted retardants because of incomplete wash-off. Some inhibitors are probably more effective than others when the retardant is diluted.

e.   Corrosion Fatigue Studies - By themselves, the base retardant solutions significantly increase susceptibility to corrosion fatigue. The relative effectiveness of each candidate inhibitor in reducing corrosion fatigue susceptibility should be determined.

f.   Inhibitor Combination Studies - Optimization of inhibitor treatment for each base retardant might require a combination of chemical inhibitors. Certain inhibitors are advantageous in preventing corrosion on certain alloys. By combining inhibitors, a retardant formulation could be derived which would be non-corrosive to all alloys.

7.   Protective Coating Evaluation

Table XVII presents the coatings selected for testing according to generic type. All of the coatings are commercially available. Coating systems 1 through 10 are widely used maintenance coatings. Coating 11 was included for possible use only on the interior of steel storage tanks.

A majority of the selected coatings failed over the course of the test period. Essentially, only two coating systems (coal tar-epoxy and amine-epoxy) performed acceptably in all three of the test solutions. The polyamide-epoxy failed in the 15% ammonium sulphate solution but exhibited very good performance in the other two test solutions. The asphalt-epoxy failed in 15% DAP, but performed well in the other solutions. All other coatings systems were unacceptable.

Tables XVIII thru XX summarize coating performance for each system. The ratings are based both on visual inspection and electrical impedance measurements.

The results predicted by the electrical impedance measurements correlate well with visual observation. Figures 32 thru 34 show the change in effective coating thickness for each coating exposed in each of the retardants over the test period. The change in effective coating thickness with time is determined periodically by measuring the electrical capacitance of the coated panels.

Figures 35 thru 37 present the electrical resistance data plotted over the test period. A decrease in coating resistance is usually indicative of coating failure.

From the results of the laboratory tests on coatings, it appears that the epoxy coatings should be specified for use as maintenance coatings in fire retardant mixing plants. All of the other coatings would provide less than adequate service. The gross deterioration of most of the maintenance coatings tested in the laboratory correlates with the deterioration which was observed on inspection trips.

TABLE I - Alloys Selected For Laboratory Testing

	Alloy	Typical Use
1.	2024-T3 Aluminum	Aircraft "skin", tanks, gates
2.	6061-T6 Aluminum	Tanks, gates, torque tubes
3.	7075-T6 Aluminum	Aircraft structural members such as spars; tanks; gates; torque tube
4.	2024-T3 Alclad Aluminum	Aircraft "skin", tanks, gates
5.	SAE 4130 Steel	Aircraft structural members such as spars, wheel treadles, torque tubes
6.	Type 304 Stainless Steel	Fasteners, control cables
7.	Type 410 Stainless Steel	Fasteners
8.	Naval Brass	Turnbuckles, cable clamps, valves, filler caps
9.	Magnesium (AZ 31 B)	Wheel rims
10.	Galvanized 1010 Steel	Control cables

TABLE II - Fire Retardants Selected For Laboratory Testing

	Retardant	Type of Use	Manufacturer/Supplier
1.	Phos-Chek ® XA	Aerial	Monsanto
2.	Phos-Chek ® 259	Ground & Aerial	Monsanto
3.	Fire-Trol ® 100	Aerial	Chemonics
4.	Fire-Trol ® 931-D* (Liquid Concentrate)	Aerial	Chemonics
5.	Fire-Trol ® 931-L* (Liquid Concentrate)	Aerial	Chemonics
6.	Pyro (Liquid Ammonium Pyrophosphate)	Aerial & Ground	TVA

*   Fire-Trol 931-D and 931-L are similar in formula except for corrosion inhibitors. Both retardants are formulated with Allied 10-34-0 at the same concentration. Fire-Trol 931-L replaced 931-D during the course of the test program. Fire-Trol 931-D was used only for the total immersion tests. Fire-Trol 931-L was used in all other tests.

TABLE III - General Corrosion Rates (MPY)
Determined by Weight
Loss Measurements

TOTAL IMMERSION TEST (2 MONTHS)

	304 SS	410 SS	BRASS	2024 AL	2024 ALC	6061 AL	7075 AL	4130 STEEL	ZINC	MAG
Phos-Chek XA	.0012	.0072	.0165	1.533	1.431	1.222	1.494	.5673	2.049	.7265
Fire-Trol 100	<.005	.0150	.1248	.0246	.0105	.0140	.0265	.5310	1.076	>100.0
Phos-Chek 259	.0054	.0223	.2716	.2865	.1441	.1019	.1494	.5303	2.498	.5318
Fire-Trol 931-D	.0096	.0054	.1743	7.113	1.857	1.530	2.108	.0898	23.29	>100.0
Pyro (11-37-0)	.0099	.0299	.1648	10.61	10.00	10.13	15.74	66.94	30.07	>100.0

ALTERNATE IMMERSION TEST (6 MONTHS)

	304 SS	410 SS	BRASS	2024 AL	2024 ALC	6061 AL	7075 AL	4130 STEEL	ZINC	MAG
Phos-Chek XA	.0043	.0087	.6081	.1061	.0909	.0736	.0711	.3017	1.333	.875
Fire-Trol 100	.0027	.0066	3.881	.1127	.0675	.0746	.0975	1.249	.7309	>100.0
Phos-Chek 259	.0019	.0087	12.48	.0782	.0497	.0584	.0782	2.173	6.234	.120
Fire-Trol 931-L	.0026	.0097	.7800	1.363	.5419	.5038	.7664	.2563	6.383	>100.0
Pyro (11-37-0)	.0047	.0015	3.000	4.387	4.063	4.543	5.234	43.99	17.58	>100.0

TABLE IV - General Corrosion Rates (MPY) Determined
By Linear Polarization Measurements Over
A Period of (2) Months

		304 SS	410 SS	BRASS	2024 AL	2024 ALC	6061 AL	7075 AL	4130 STEEL	ZINC	MAG
Phos-Chek XA	Initial	.0125	.0199	.0212	2.880	2.870	2.27	2.27	1.908	3.011	.2652
		.0172	.0380	.0116	1.567	2.099	1.190	1.274	2.091	2.137	.1343
		.0075	.0300	.0138	1.389	2.099	1.357	1.126	1.855	1.489	.0482
	thru	.0131	.1101	.0095	1.102	1.601	1.166	1.038	1.276	.9938	.0546
		.0035	.0252	.0068	1.083	1.740	1.174	.984	.7331	.9107	.0412
		.0014	.0693	.0070	.980	.9697	.4303	.6755			.0178
				.0040	.6844	.3322	.227	.4457			.0258
	Final				.4086	.1780					
	Average	.0092	.0468	.0105	1.262	1.466	1.116	1.116	1.573	1.706	.0637
Fire-Trol 100	Initial	.0233	.0019	.4318	.0676	.0509	.0383	.045	.4588	.5935	108.1
		.0164	.0048	1.08	.0815	.0473	.0313	.025	.2933	.6183	
		.0030	.0030	.6751	.0335	.0358	.0204	.0190	.2876	.5219	
	thru	.0041	.0024	.4812	.0057	.0047	.0047	.0042	.2848	.9694	
		.0038	.0026	.5685	.0032	.0024	.0024	.0016	.1076	.9146	
		.0166	.0006	.0738	.0008	.0029	.0044		.2397	.6560	
	Final									.4641	
	Average	.0112	.0026	.5517	.0321	.0240	.0169	.0064	.2766	.6766	>100
Phos-Chek 259	Initial	.0173	.0145	.2025	.0088	.0079	.0048	.0132	.8319	2.789	.0371
		.0090	.0222	.1705	.0154	.0059	.0030	.0044	.7172	2.892	.0244
		.0053	.0037	.1044	.0099	.0033	.0013	.0028	.9506	2.717	.0301
	thru	.0023	.0102	.2430	.0088	.0037	.0012	.0023	1.206	1.988	.0203
		.0013	.0039	.2578	.0277	.0008	.0013	.0006	.7785	1.011	.0110
			.0037	.4135			.0225	.0009	.6747	.8151	.0213
	Final							.0013	.8435	.5759	
	Average	.0070	.0097	.2320	.0141	.0074	.0021	.0041	.8575	1.627	.0240

		304 SS	410 SS	BRASS	2024 AL	2024 ALC	6061 AL	7075 AL	4130 STEEL	ZINC	MAG
Fire-Trol 931-D	Initial	.0081	.1663	.1665	.1068	.1828	.1026	.0749	.0266	>100	347.8
		.0069	.1101	.1080	4.986	1.763	.8014	.8565	.0456	18.65	
	thru	.0051	.0748	.1865	5.488	1.325	.9788	1.031	.0140	2.283	
		.0031	.0058	.1163	4.333	.6640	.7945	.9794	.0195	1.197	
		.0010	.0014	.1108	3.080	.5517	.7822	.6659		.6921	
	Final	.0064	.0043	.0871	2.263	.7676	.7377	.9389			
	Average	.0051	.0605	.1292	3.376	.6757	.6995	.7578	.0264	14.75	>100
Pyro (11-37-0)	Initial	.0179	.0442	2.377	4.315	3.621	3.061	3.813	18.9	>100	53.12
		.2674	.275	.1661	8.198	6.804	6.664	8.706	115.6	23.66	
		1.419	.1756	.0222	4.862	5.887	3.014	8.162	122.4	14.63	
	thru	.0171	.3436	.0216	6.076	7.101	5.095	9.795		12.49	
		.0255	.1116	.0240	3.071	5.234	3.095	6.928		11.73	
		.0269	.0814	.0582	3.284	3.851	2.352	4.255		14.36	
		.0138	.0447	.0275	1.839	2.718	.8652	1.781		2.273	
	Final				2.548						
	Average	.2554	.1537	.3652	4.274	5.031	3.449	6.206	85.63	14.13	>100

TABLE V - Comparison of General Corrosion Rates Determined By Weight Loss and Linear Polarization Methods

	PHOS-CHEK XA		FIRE-TROL 100		PHOS-CHEK 259		FIRE-TROL 931-D		PYRO (11-37-0)	
	WEIGHT LOSS	LINEAR POLAR*	WEIGHT LOSS	LINEAR POLAR*	WEIGHT LOSS	LINEAR POLAR*	WEIGHT LOSS	LINEAR POLAR*	WEIGHT LOSS	LINEAR POLAR*
2024 AL	1.533	1.262	.0246	.0321	.2865	.0141	7.113	3.376	10.61	4.274
2024 ALC	1.431	1.466	.0105	.0240	.1441	.0074	1.857	.6757	10.00	5.031
6061 AL	1.222	1.116	.0140	.0169	.1019	.0021	1.530	.6995	10.13	3.449
7075 AL	1.494	1.116	.0265	.0064	.1494	.0041	2.108	.7578	15.74	6.206
NAVAL BRASS	.0165	.0105	.1248	.5517	.2716	.2320	.1743	.1292	.1648	.3652
4130 STEEL	.5673	1.573	.5310	.2766	.5303	.8575	.0898	.0264	66.94	85.63
ZINC	2.049	1.706	1.076	.6766	2.498	1.627	23.29	14.75	33.07	14.13
304 SS	.0012	.0092	.0046	.0112	.0054	.0070	.0096	.0051	.0099	.2554
410 SS	.0072	.0468	.0150	.0026	.0223	.0097	.0054	.0605	.0299	.1537
MAG	.7265	.0637	>100	>100	.5318	.0240	>100	>100	>100	>100

*Average rate calculated from several measurements made during 60-day test period.

TABLE VI - Average Corrosion Potentials Over 2 Month Exposure Period

CORROSION POTENTIALS VS Ag/AgCl, VOLTS

ALLOY -	PYRO	FIRE-TROL 931-D	PHOS-CHEK 259	FIRE-TROL 100	PHOS-CHEK XA
Naval Brass	-.36	-.21	-.34	-.11	-.28
304 SS	-.37	+.04	-.08	-.05	-.17
410 SS	-.57	-.06	-.14	+.07	-.22
Zinc	-.76	-.63	-.90	-.97	-.90
4130 Steel	-.71	-.17	-.71	-.61	-.71
6061 AL	-.86	-.91	-.70	-.62	-.94
7075 AL	-.80	-.86	-.30	-.70	-.95
2024 ALC	-.76	-.86	-.56	-.57	-.95
2024 AL	-.75	-.81	-.30	-.55	-.92

TABLE VII - The Five Worst Galvanic Corrosion Rates For
Each Fire Retardant

RETARDANT	CATHODE	E_C VOLTS	ANODE	E_C VOLTS	ΔE_C VOLTS	I_C $\mu a/cm^2$	CORROSION RATE (MPY)
Fire-Trol 931-L							
1.	Brass	-.10	2024 Al	-.71	.61	5.0	4.49
2	410 SS	-.18	2024 Al	-.71	.89	4.0	3.60
3	Brass	-.10	4130 Stl	-.61	.51	6.5	3.02
4	Brass	-.10	7025 Al	-.74	.64	4.9	2.14
5	410 SS	+.18	4130 Stl	-.61	.79	3.8	1.76
Fire-Trol 100							
1	Brass	+.04	Zinc	-.97	1.02	100+	59.10+
2	Brass	+.04	4130 Stl	-.65	.69	37.0	17.70
3	2024 Al	-.11	Zinc	-.97	.88	11.5	6.80
4	304 SS	+.05	Zinc	-.97	1.02	11.0	6.50
5	6061 Al	-.02	Zinc	-.97	.95	4.2	2.48
Phos-Chek XA							
1	410 SS	-.16	Zinc	-.88	.72	17.5	10.34
2	Brass	-.34	Zinc	-.88	.54	11.0	6.50
3	410 SS	-.16	4130 Stl	-.66	.50	9.2	4.27
4	Brass	-.34	4130 Stl	-.66	.32	8.5	3.94
5	410 SS	-.16	7075 Al	-.91	.75	5.8	2.53
Phos-Chek 259							
1	Brass	-.35	Zinc	-.84	.49	7.0	4.14
2	Brass	-.35	4130 Stl	-.63	.28	8.5	3.94
3	304 SS	-.02	Zinc	-.84	.82	4.2	2.48
4	410 SS	-.02	Zinc	-.84	.82	3.9	2.31
5	304 SS	-.02	4130 Stl	-.63	.61	3.2	1.48

RETARDANT	CATHODE	E_c VOLTS	ANODE	E_c VOLTS	ΔE_c VOLTS	I_c $\mu a/cm^2$	CORROSION RATE (MPY)
Pyro 11-37-0							
1	Brass	-.37	2024 Al	-.72	.35	8.5	7.64
2	Brass	-.37	Steel	-.68	.31	10.0	5.91
3	4130 Stl	-.68	7075 Al	-.75	.03	7.0	3.06
4	4130 Stl	-.68	6061 Al	-.81	.03	7.0	3.06
5	304 SS	-.38	6061 Al	-.81	.43	5.0	2.19

TABLE VIII - Results of Tensile Tests On Different Alloys Included In Laboratory Program

ALLOY	ULTIMATE TENSILE STRENGTH, psi	.2% OFFSET YIELD STRENGTH, psi
2024-T3 Al	64,550	45,750
2024-T3 Alclad	68,400	48,700
6061-T6 Al	45,250	39,900
7075-T6 Al	78,200	69,600
Magnesium	44,300	39,350
Galvanized 1010 Steel	42,500	32,250
Naval Brass	62,600	35,300
4130 Steel	186,000	175,000
410 SS	181,000	150,000
304 SS	83,500	42,600

TABLE IX - Results of DCB Stress Corrosion Cracking Tests

RETARDANT	ALLOY	CRACK GROWTH	K_{IC}	K_{ISCC}	% REDUCTION IN K_{IC}
Phos-Chek XA	6061 Al	.129	75.0	52.0	30%
Phos-Chek 259	6061 Al	.065	217.5	192.5	11%
Phos-Chek XA	7075 Al	.007	35.5	35.5	<1%
Phos-Chek 259	7075 Al	.042	42.6	22.8	46%
Fire-Trol 931-L	2024 Al	.079	132.5	121.4	6%
Pyro	2024 Al	.043	132.5	99.6	24%
Fire-Trol 931-L	4130 Stl	.976	339.	162.9	52%
Phos-Chek XA	4130 Stl	1.12	231	115.1	50%
Pyro	4130 Stl	.537	417	266.8	36%
Fire-Trol 100	4130 Stl	.289	186	146.8	21%
Phos-Chek 259	4130 Stl	.39	567	471.2	16%
Pyro	410 SS	.15	53.5	-	-
Phos-Chek XA	Naval Brass	.452	-	-	-
Fire-Trol 100	Naval Brass	.422	-	-	-
Pyro	Naval Brass	.028	-	-	-

<div align="center">

TABLE X - Chemicals Selected For Testing As
Candidate Corrosion Inhibitors

</div>

CHEMICAL	FORMULA	REFERENCES
Sodium Mercaptobenzothiazole	$NaC_7H_4NS_2$	1,2,3,4
Sodium Dichromate	$Na_2Cr_2O_7 \cdot 2H_2O$	3,5,8,9
Sodium Flurosilicate	Na_2SiF_6	3,4,5
Thiourea	NH_2CSNH_2	2,5,10
Ammonium Fluoride	NH_4F	8
Sodium Nitrite	$NaNO_2$	4,5
Dimethylamine	$(CH_3)_2NH$	4,5,11
Aniline Sulfate	$(C_6H_5NH_2)_2 \cdot H_2SO_4$	5,13,14
Ammonium Thiocyanate	NH_4SCN	2,12
Sodium Ferrocyanide	$Na_4Fe(CN)_6 \cdot H_2O$	6,7,15

<div align="center">

REFERENCES FOR TABLE X

</div>

1. Inhibition of Metallic Corrosion in Aqueous Media,
    CORROSION, 12, 23t (1956).

2. Inhibiting Mild Steel in Nitrogen Fertilizers, MATERIALS
    PROTECTION, 7, 35 (1968).

3. Burns, R. M. and Bradley, W. W., PROTECTIVE COATINGS FOR
    METALS, 3rd Ed., Reinhold Publ. Corp., N.Y., 1967, p. 83.

4. Brooke, Maxey, Corrosion Inhibitor Checklist, CHEMICAL
    ENGINEERING (1962) Feb., p. 83.

5. Eldredge, G. G. and Mears, R. B., Inhibitors of Corrosion
    of Aluminum, INDUSTRIAL AND ENGINEERING CHEMISTRY, 37
    (1945) August, p. 736.

6. Wilson, C. L. and Oates, J. A., CORROSION AND THE MAINTENANCE
    ENGINEER, Hart Publishing Co., Inc., N.Y. (1968) p. 688.

7. Sugawara, J. and Shinodaira, J., On the Corrosion Protection of Aluminum Brass by Ferrous or Ferric Ion, J. JAPAN INST. METALS, 30, 869-873.

8. Wyma and Wagner, Aluminum Use in the Fertilizer Industry, CHEMICAL ENGINEERING PROGRESS, 60, P. 55.

9. Inhibition of Mild Steel Corrosion Under Desalination Conditions, MATERIALS PROTECTION, 9, No. 9, p. 35.

10. Negoro, K. and Hashioka, J., Inhibition of Iron Corrosion in Sulfuric Acid, J. JAPAN OIL CHEMISTS SOC., 16, No. 11, 623-625.

11. Desai, M. N. and Shah, C. B., Methylaminues as Corrosion Inhibitors for Al-57S in Hydrochloric Acid Solutions, WERKSTOFEE AND KORROSION, 21, 789-791.

12. Rana, S. L. and Desai, M. N., A Study of the Corrosion Inhibition of Copper in Potassium-Persulphate Solutions, 3rd INTERNATIONAL CONGRESS ON METALLIC CORROSION (1966).

13. Donew, L. and Boydzkiev, J., Effect of Some Organic Compounds in the Anodic Oxidation of Aluminum, J. APPLIED CHEM., USSR, 32, 2031-2034.

14. Boies, D. B. and Northan, B. J., Aluminum Corrosion, Possible Mechanisms of Inhibition, MATERIALS PROTECTION, 7, p. 27.

15. Hersh, P. etal, An Experimental Survey of Rust Preventatives in Water, J. APPLIED CHEM. 11, 246-271.

TABLE XI - Corrosion Rates* In Diammonium Phosphate For Different Inhibitors

ALLOY	2024 AL	2024 ALC	6061 AL	7075 AL	Mg.	NAVAL BRASS	GALV. 1010	4130 STEEL	304 SS	410 SS
INHIBITOR				CORROSION RATE (MILS PER YEAR)						
Thiourea	19.6	19.6	9.2	10.4		.53	.115	.858	.025	.008
Dimethylamine	20.1	18.55	9.8	12.7		.756	.0814	2.9	.0065	.0104
Ammonium Thiocyanate	24.27	26.56	11.87	18.63		.847	.623	.539	.054	.045
Sodium Fluorosilicate	2.87	15.15	1.52	1.89	.806	46.3	3.58	7.35	.0741	.255
Sodium Dichromate	.043	.046	.022	.010	.0097	.615	.0358	.193	.0023	
Ammonium Fluoride	.755	.61	.174	.255		2.88	1.56	.21	.0038	.0044
Sodium MBT	12.99	9.42	3.92	4.77	.0062	.303	.360	.331	.0022	.0168
Sodium Nitrite	20.5	10.34	3.36	11.8	.0064	3.77	.317	.535	.0044	.026
Aniline Sulfate	26.8	15.2	6.52	13.7		2.03	2.22	1.07	.067	.0348
Sodium Ferrocyanide	24.8	30.22	9.17	4.29		12.6	.578	1.70	.015	.520

*Determined by polarization measurements

TABLE XII - Corrosion Rates* In Ammonium Sulfate For Different Inhibitors

ALLOY	2024 AL	2024 ALC	6061 AL	7075 AL	Mg.	NAVAL BRASS	GALV. 1010	4130 STEEL	304 SS	410 SS
INHIBITOR	CORROSION RATE (MILS PER YEAR)									
Thiourea	.921	.921	.491	.356		6.17	23.97	2.19	.0113	.051
Dimethylamine	.143	.152	.019	.036		1.08	.477	.971	.080	.065
Ammonium Thiocyanate	.065	.224	.098	.179	671.7	.167	2.52	.722	.011	.21
Sodium Fluorosilicate	1.98	5.87	3.25	1.35		2.08	48.09	46.4	.0073	1.28
Sodium Dichromate	1.11	.917	.042	.089		.78	.20	.125	.040	.032
Ammonium Fluoride	.484	1.49	.619	4.31		.294	9.04	.437	.0092	.403
Sodium MBT	.161	.143	.028	.035		.216	.271	.306	.018	.098
Sodium Nitrite	.424	.0092	.0024	.169		.177	20.7	19.1	.0069	.69
Aniline Sulfate	.167	.0402	.033	.067	.193	1.17	21.95	.655	.0044	.396
Sodium Ferrocyanide	.088	.110	.020	.017		.268	.75	.834	.055	.055

*Determined by polarization measurements

TABLE XIII - Corrosion Rates* In Liquid Ammonium Polyphosphate For Different Inhibitors

ALLOY	2024 AL	2024 ALC	6061 AL	7075 AL	Mg.	NAVAL BRASS	GALV. 1010	4130 STEEL	304 SS	410 SS
INHIBITOR	CORROSION RATE (MILS PER YEAR)									
Thiourea	4.60	7.57	3.83	2.14	1.76	6.14	7.18	1.73	1.04	.084
Dimethylamine	34.37	24.57	3.13	7.84		1.87	2.65	1.16	.024	.0256
Ammonium Thiocyanate	.422	1.08	.57	.795	1.75	1.32	.979	1.31	.0029	.208
Sodium Fluorosilicate	14.89	1.69	.784	9.78		5.36	1.32	1.44	.045	.150
Sodium Dichromate	1.83	.353	.051	.056	268.7	.469	11.9	.108	.0038	.146
Ammonium Fluoride	251.3	127.1	68.9	85.4		5.72	3.18	1.39	.138	.095
Sodium MBT	.511	.975	.076	.751	2.84	2.45	3.35	1.89	.0103	.177
Sodium Nitrite	.795	1.51	2.45	1.52	2.38	6.95	35.8	1.08	.0047	.306
Aniline Sulfate	19.16	3.04	2.21	11.59		2.78	1.62	1.46	.029	.059
Sodium Ferrocyanide	1.45	1.28	.862	1.32		.324	.442	.520	.026	.076

*Determined by polarization measurements

TABLE XIV - General Corrosion Rates For 3 Best Inhibitors Over 30 Day Test Period

ALLOY		2024	2024 ALC	6061	7075	MAG	NAVAL BRASS	ZINC	4130 STEEL	304 SS	410 SS
INHIBITOR											
1% Sodium Dichronate In DAP.	Wt. Loss*	.0342	.022	.037	-	.168	.034	.272	.031	-	-
	Initial**	.893	1.96	.400	.750	9.05	.480	.274	.046	.069	.010
	14 Days**	.076	.143	.011	.036	.086	1.63	.098	.019	.017	.009
	Final**	.060	.090	.008	.022	.144	1.41	.095	.017	.185	.134
1% Sodium Ferrocyanide In Ammonium Sulfate	Wt. Loss	.013	.023	.009	.027	-	.002	.264	.119	.003	.033
	Initial	.090	.148	.003	.095	774.9	.467	10.6	7.09	.011	.016
	14 Days	.001	.003	.0002	.003	-	.25	5.05	3.96	.006	.008
	Final	.003	.005	.001	.003	-	.128	7.81	3.57	.012	.017
1% Ammonium Thiocyanate In Poly - phosphate	Wt. Loss	.227	.256	.201	.245	13.6	.040	.406	.308	-	.069
	Initial	11.72	9.06	4.99	5.32	20.9	2.57	10.2	3.69	.030	.064
	14 Days	.106	.060	.061	.021	5.62	.256	.047	.288	.020	.297
	Final	.041	.099	.051	.037	5.22	.299	.589	.277	.035	.231

* Corrosion rate determined by weight loss over 30-day period.

** Corrosion rate determined by linear polarization measurements; in order, initial, 14-day, and final measurements over a 30-day period.

TABLE XV - Galvanic Corrosion Rates in Selected Inhibitors

RETARDANT	CATHODE	E_c	ANODE	E_c	ΔE_c	I_c	CORROSION RATE (MPY)
1% Sodium Ferrocyanide In Ammonium Sulfate	NAVAL BRASS	-.18	7075 ALUMINUM	-.27	.09	.145	.062
1% Sodium Ferrocyanide In Ammonium Sulfate	410 SS	-.05	2024 ALCLAD	-.28	.33	.23	.20
1% Sodium Dichromate In Diammonium Phosphate	410 SS	-.24	7075 ALUMIMUM	-.64	.40	2.0	.87
1% Ammonium Thiocyanate In Polyphosphate	NAVAL BRASS	-.29	2024 ALUMINUM	-.39	.10	.39	.35

TABLE XVI - Results of DCB Stress Corrosion Corrosion
Cracking Tests for Inhibitor Screening Phase

RETARDANT	INHIBITOR	ALLOY	CRACK GROWTH OVER 1000 HOURS
Ammonium Polyphosphate	Ammonium Thiocyanate	2024 Aluminum	.15"
Diammonium Phosphate	Sodium Dichromate	7075 Aluminum	.25"
Ammonium Sulfate	Sodium Ferrocyanide	4130 Steel	1.08"

TABLE XVII

COATINGS SELECTED FOR LABORATORY TESTING

NO.   GENERIC TYPE

1. Rust - Penetrating Primer
   Modified - oil Alkyd Topcoat

2. Modified Vinyl Primer
   Vinyl Topcoat

3. Epoxy - Polyamide Primer
   Epoxy - Polyamide Topcoat

4. Epoxy - Amine Primer
   Epoxy - Amine Topcoat

5. Epoxy - Coal Tar Primer
   Epoxy - Coal Tar Topcoat

6. Epoxy - Ester Primer
   Epoxy - Ester Topcoat

7. Modified Vinyl Primer
   Modified Acrylic Topcoat

8. Epoxy - Polyamide Primer
   Acrylic Latex Topcoat

9. Rust - Penetrating Primer
   Phenolic Topcoat

10. Flake - filled Polyester Primer
    Flake - filled Polyester Topcoat

11. Bituminous Asphaltic Epoxy

TABLE XVIII - General Description of Coating Performance
In Diammonium Phosphate (15%, by weight)

| NO.	COATING	REMARKS
1.	Rust - Penetrating Primer Modified - oil Alkyd Topcoat	Poor (Blistering and coating disbondment)
2.	Modified Vinly Primer Vinyl Topcoat	Poor (Blistering)
3.	Epoxy - Polyamide Primer Epoxy - Polyamide Topcoat	Very Good
4.	Epoxy - Amine Primer Epoxy - Amine Topcoat	Very Good
5.	Epoxy - Coal Tar Primer Epoxy - Coal Tar Topcoat	Very Good
6.	Epoxy - Ester Primer Epoxy - Ester Topcoat	Fair (Blistering)
7.	Modified Vinyl Primer Modified Acrylic Topcoat	Poor (Blistering and coating disbondment)
8.	Epoxy - Polyamide Primer Acrylic Latex Topcoat	Poor (Blistering, cracking and disbondment)
9.	Rust - Penetrating Primer Phenolic Topcoat	Poor (Blistering and discoloration)
10.	Flake - filled Polyester Primer Flake - filled Polyester Topcoat	Poor (Blistering)
11.	Bituminous Asphaltic Epoxy	Poor (Blistering)

TABLE XIX - General Description of Coating Performance
             in Pyro (10-34-0, diluted 4:1)

NO.	COATING	REMARKS
1.	Rust - Penetrating Primer Modified - oil Alkyd Topcoat	Poor (Blistering)
2.	Modified Vinyl Primer Vinly Topcoat	Fair (Blistering)
3.	Epoxy - Polyamide Primer Epoxy - Polyamide Topcoat	Very Good
4.	Epoxy - Amine Primer Epoxy - Amine Topcoat	Very Good
5.	Epoxy - Coal Tar Primer Epoxy - Coal Tar Topcoat	Very Good
6.	Epoxy - Ester Primer Epoxy - Ester Topcoat	Poor (Blistering)
7.	Modified Vinyl Primer Modified Acrylic Topcoat	Poor (Blistering)
8.	Epoxy - Polyamide Primer Acrylic Latex Topcoat	Poor (Blistering)
9.	Rust - Penetrating Primer Phenolic Topcoat	Poor (Blistering)
10.	Flake - filled Polyester Primer Flake - filled Polyester Topcoat	Poor (Disbondment)
11.	Bituminous Asphaltic Epoxy	Very Good

TABLE XX - General Description of Coating Performance In Ammonium Sulphate (15%, by weight)

NO.	COATING	REMARKS
1.	Rust - Penetrating Primer Modified - oil Alkyd Topcoat	Poor (Blistering and disbondment)
2.	Modified Vinyl Primer Vinyl Topcoat	Poor
3.	Epoxy - Polyamide Primer Epoxy - Polyamide Topcoat	Poor (Blistering and disbondment)
4.	Epoxy - Amine Primer Epoxy - Amine Topcoat	Very Good
5.	Epoxy - Coal Tar Primer Epoxy - Coal Tar Topcoat	Very Good
6.	Epoxy - Ester Primer Epoxy - Ester Topcoat	Poor (Blistering, rusting
7.	Modified Vinyl Primer Modified Acrylic Topcoat	Poor (Blistering, rusting
8.	Epoxy - Polyamide Primer Acrylic Latex Topcoat	Poor (Blistering, rusting
9.	Rust - Penetrating Primer Phenolic Topcoat	Poor (Blistering, rusting
10.	Flake - filled Polyester Primer Flake - filled Polyester Topcoat	Poor (Blistering, disbondment and rusting)
11.	Bituminous Asphaltic Epoxy	Very Good
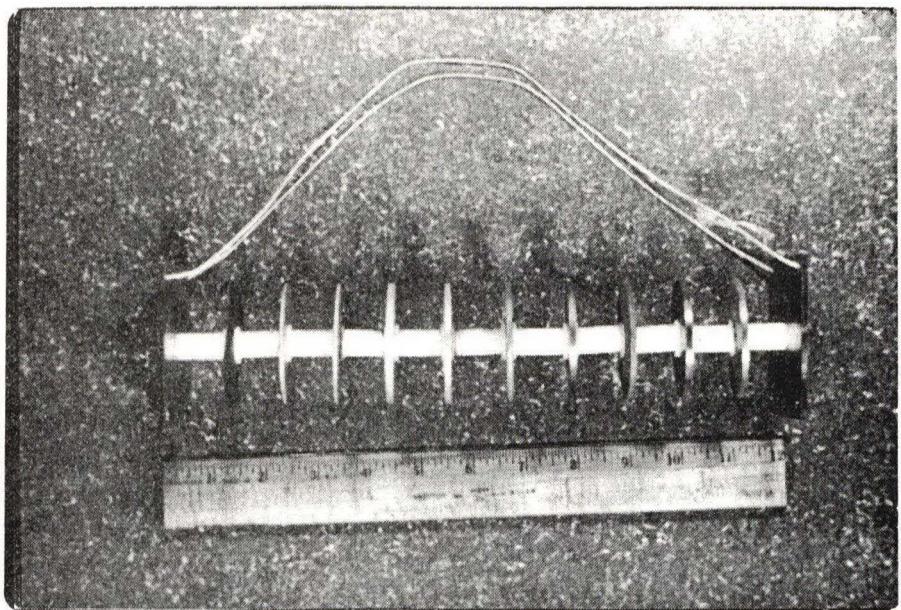
Figure 1 - Alternate Immersion Test Rack
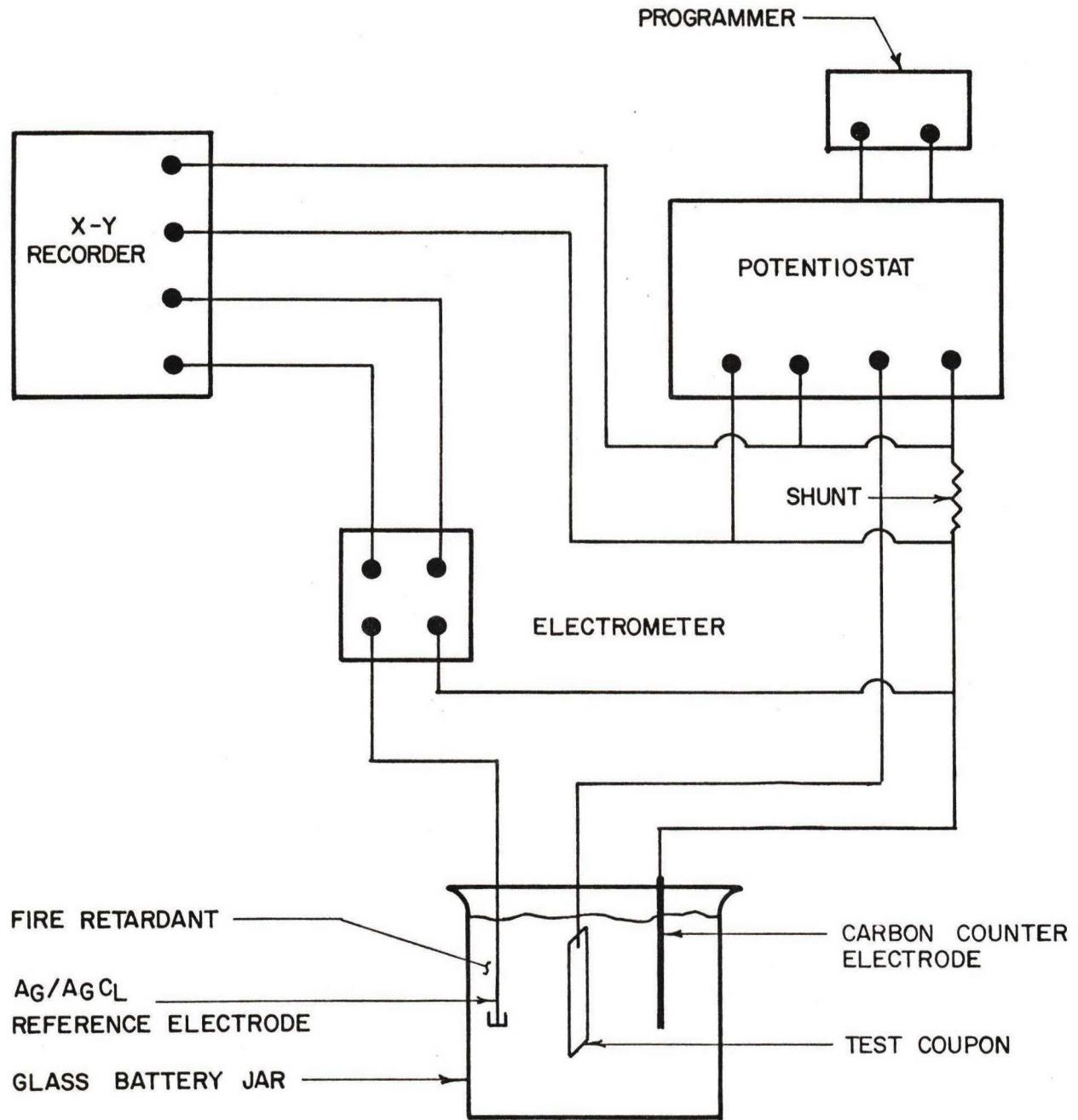
FIGURE 2 — SET-UP FOR MAKING POLARIZATION
MEASUREMENTS

MASK ENDS WITH EPOXY

1"
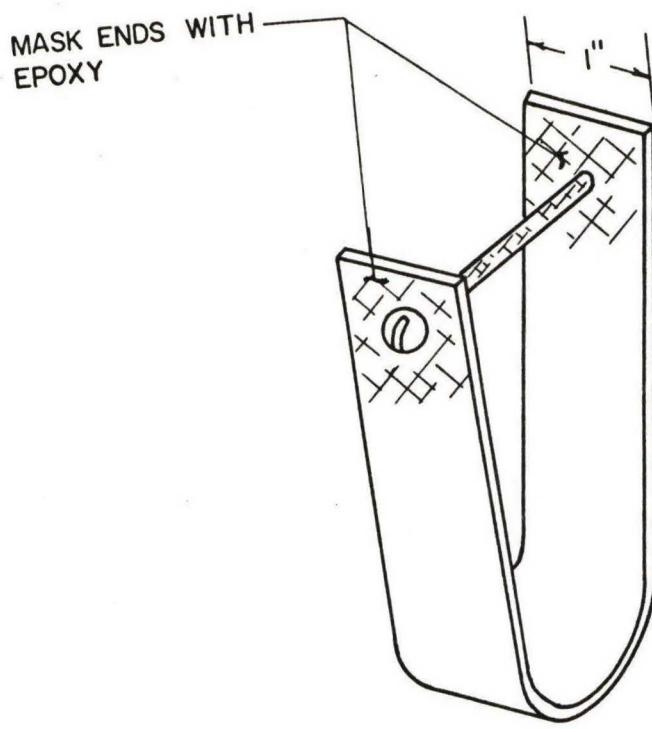
FIGURE 3 - U-BEND SPECIMEN
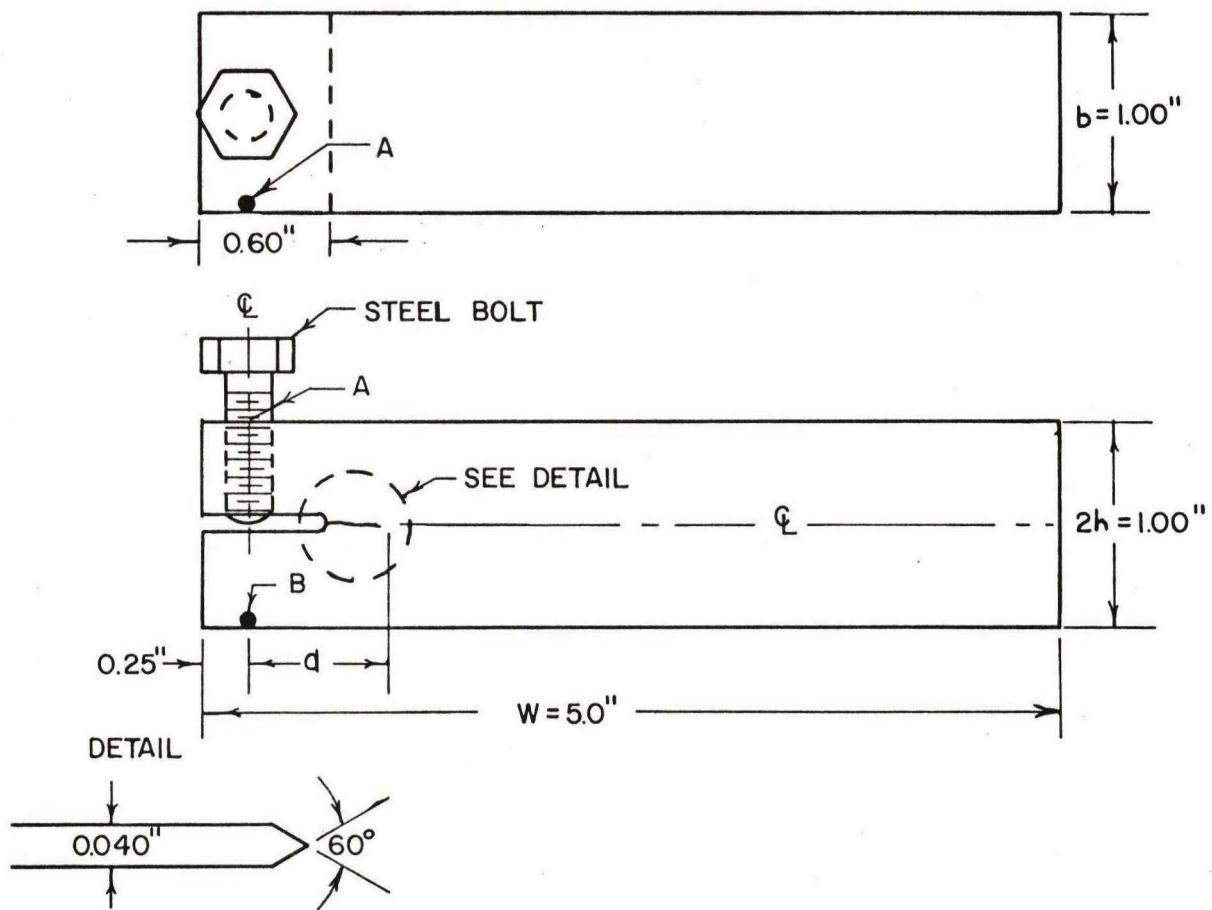
CRACK OPENING DISPLACEMENT v EQUALS THE MEASURED DEFLECTION
BETWEEN POINTS A AND B ALONG THE BOLT CENTERLINE.

FIGURE 4 - DCB SPECIMEN USED FOR STRESS CORROSION TESTING

60° NOTCH

FIRE RETARDANT

TEST BEAM

SILICONE RUBBER SEALANT

POLYETHYLENE BOTTLE

DETAIL

SPEED CONTROL

CYCLE COUNTER

CRANK

EXTENSION BAR

VISE

TEST SPECIMEN

FIRE RETARDANT, SEE DETAIL
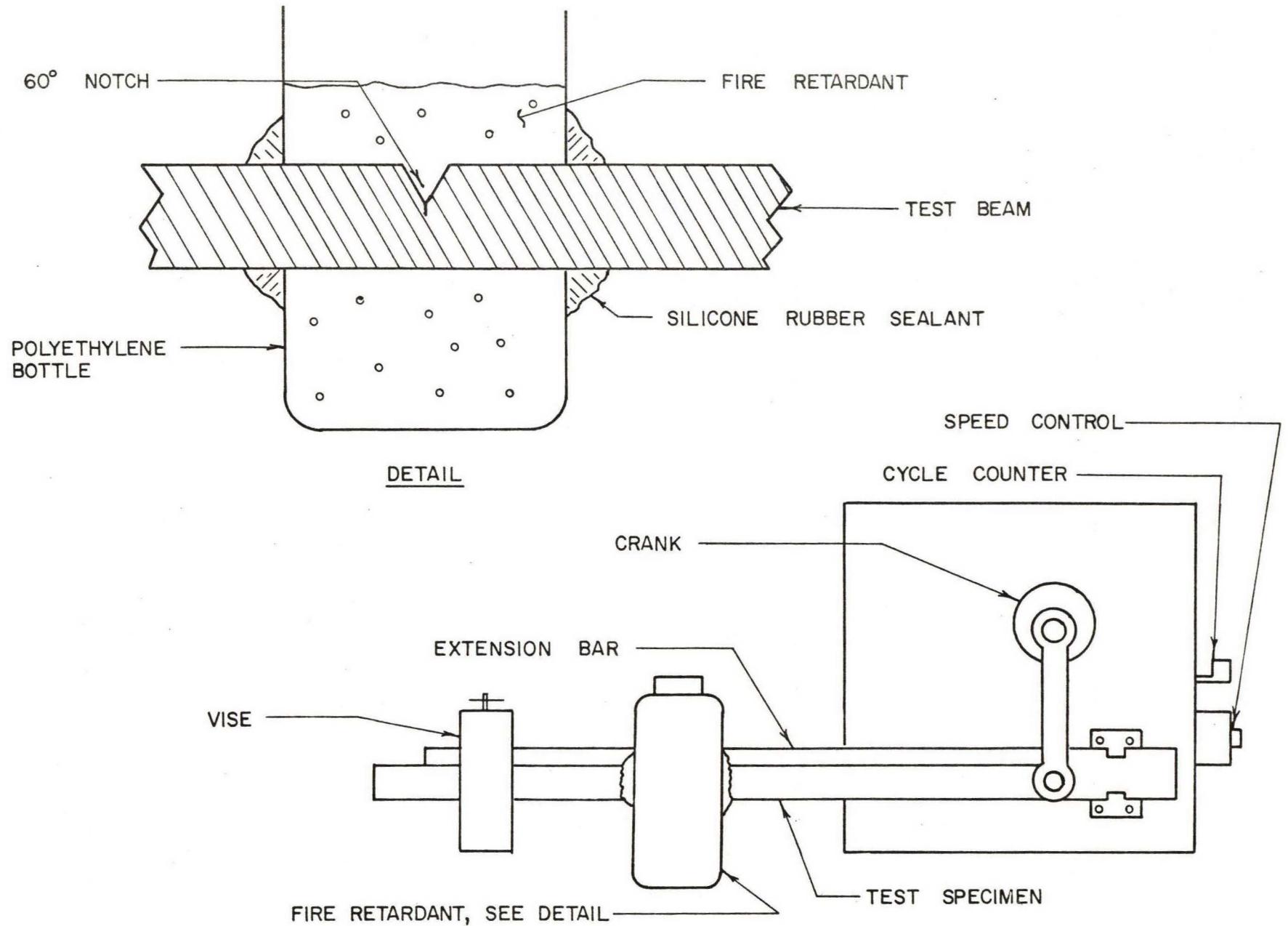
FIGURE 5 - TYPICAL SET-UP FOR FATIGUE TESTS
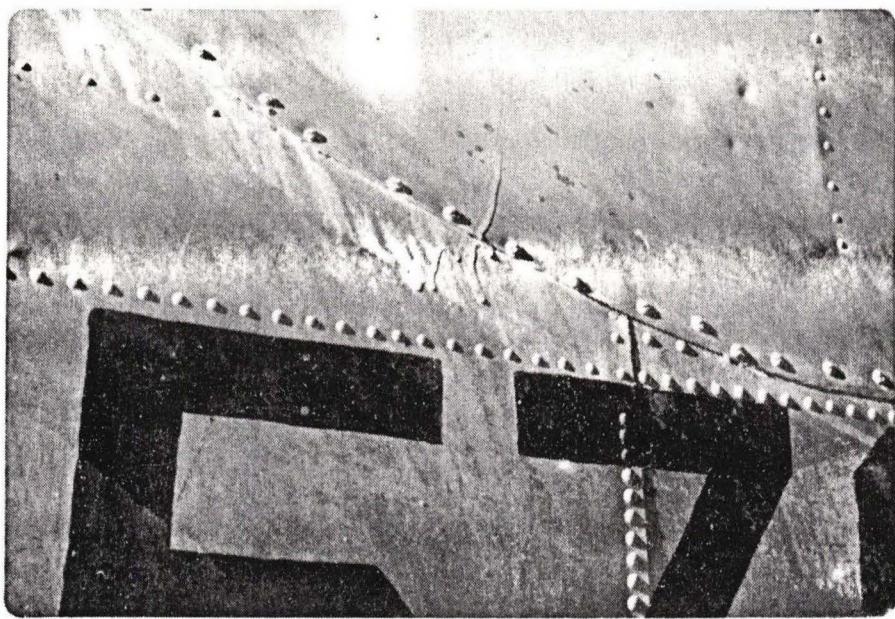
Figure 6 - Corrosion of Bolts and At Seam On
Tail of Air Tanker
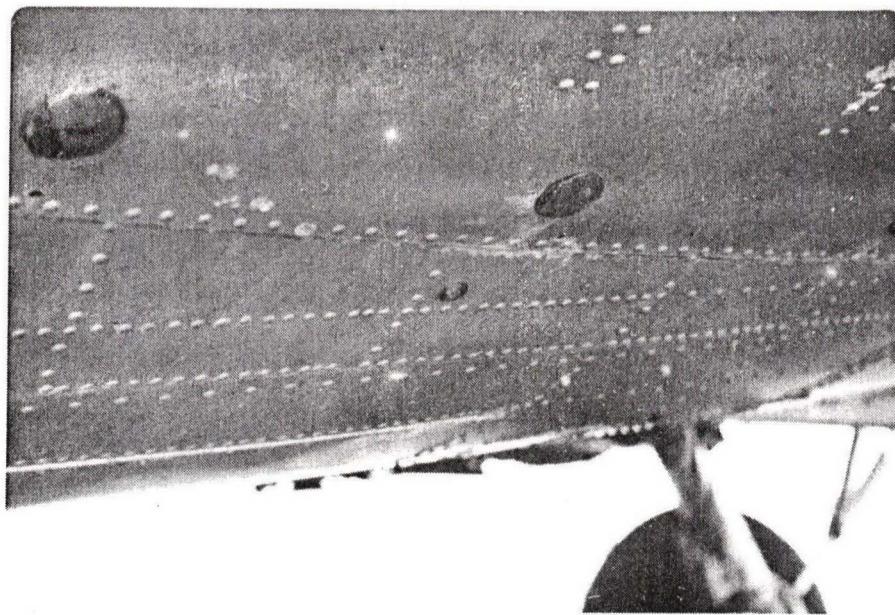
Figure 7 - Pitting Corrosion On Skin And
Corrosion At Seam on Air Tanker
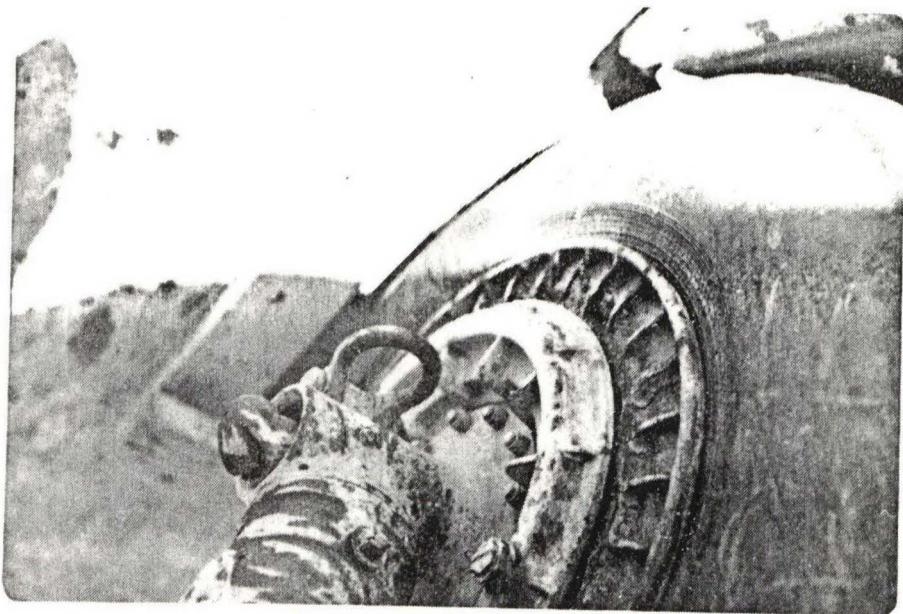
Figure 8 - Pitting Corrosion On Magnesium
Wheels of Air Tanker
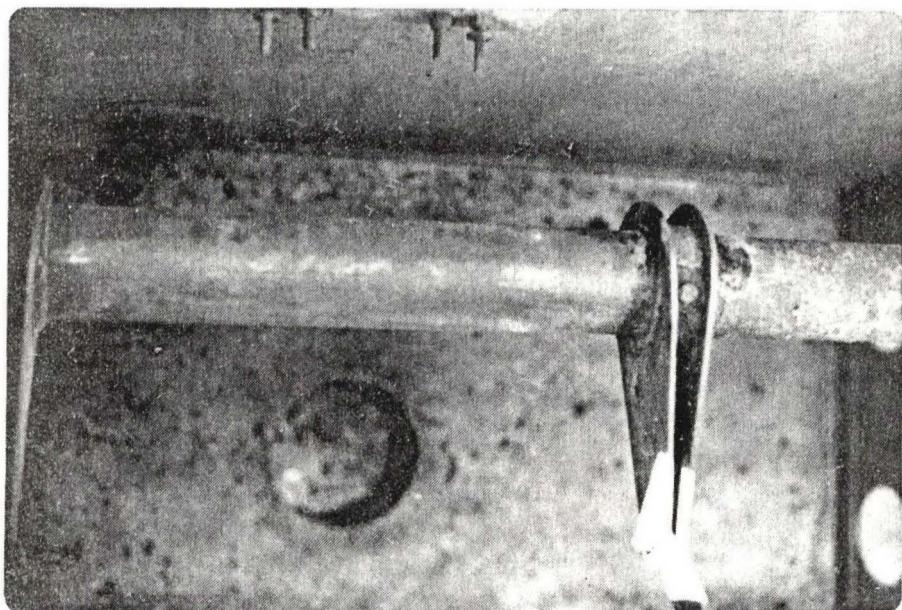
Figure 9 - Light, General Corrosion On 4130 Steel
Torque Tube In Retardant Tank Of Aircraft
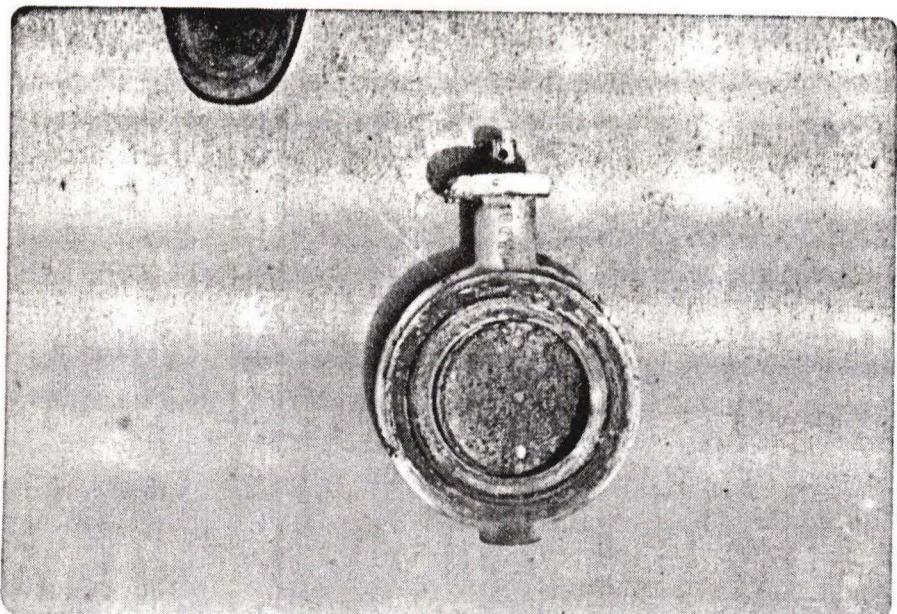
Figure 10 - Corrosion of Steel Butterfly Valve
Used in Fire Retardant Mixing Plant
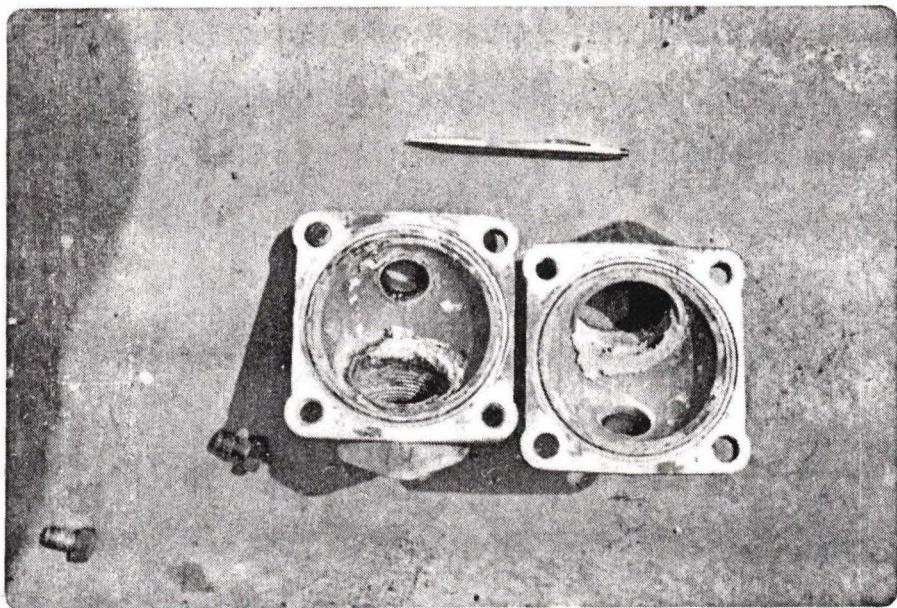
Figure 11 - Corrosion of Brass Ball Valve Used
In Fire Retardant Mixing Plant
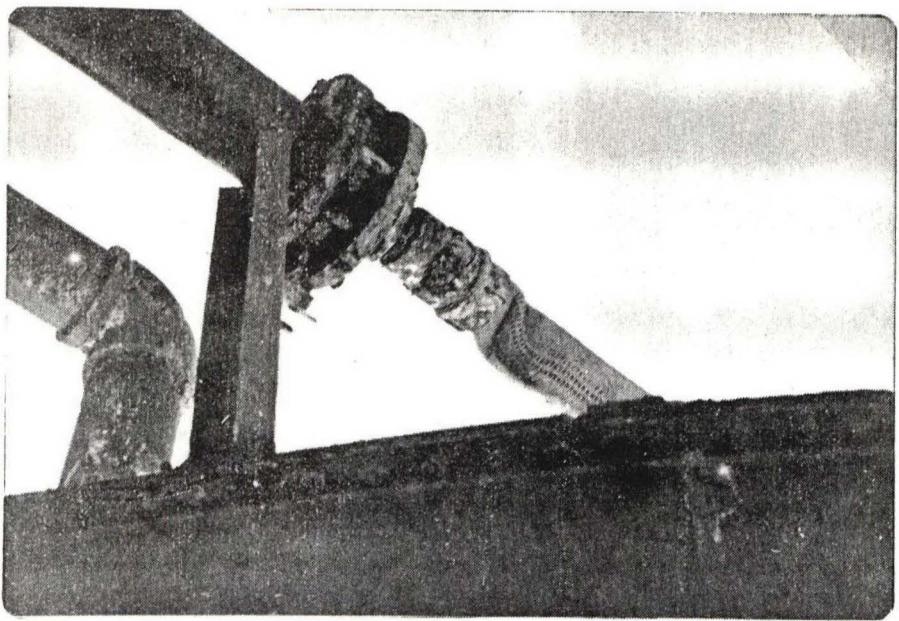
Figure 12 - Corrosion of Brass Hose Coupling In
Fire Retardant Mixing Plant
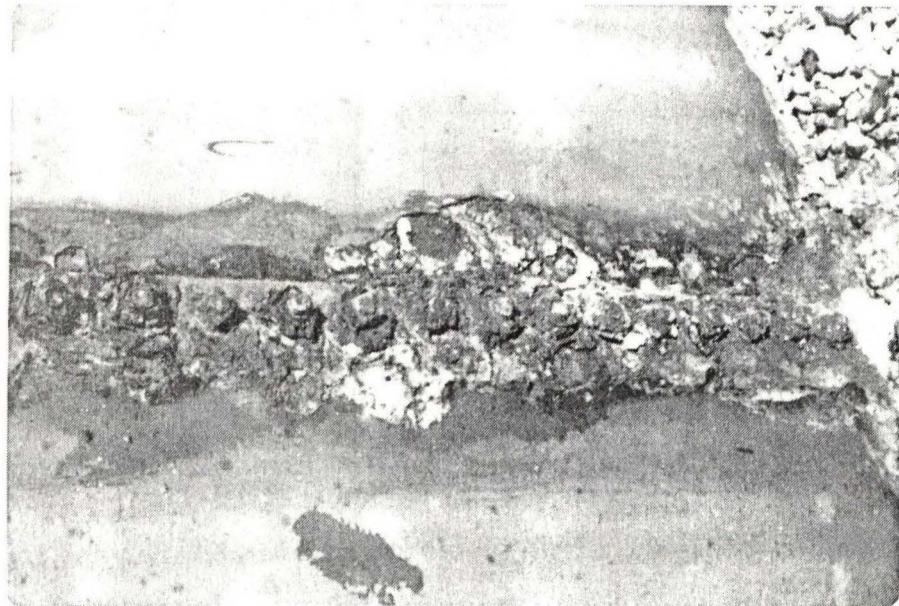
Figure 13 - Corrosion At Steel Storage Tank Seam
In Fire Retardant Mixing Plant
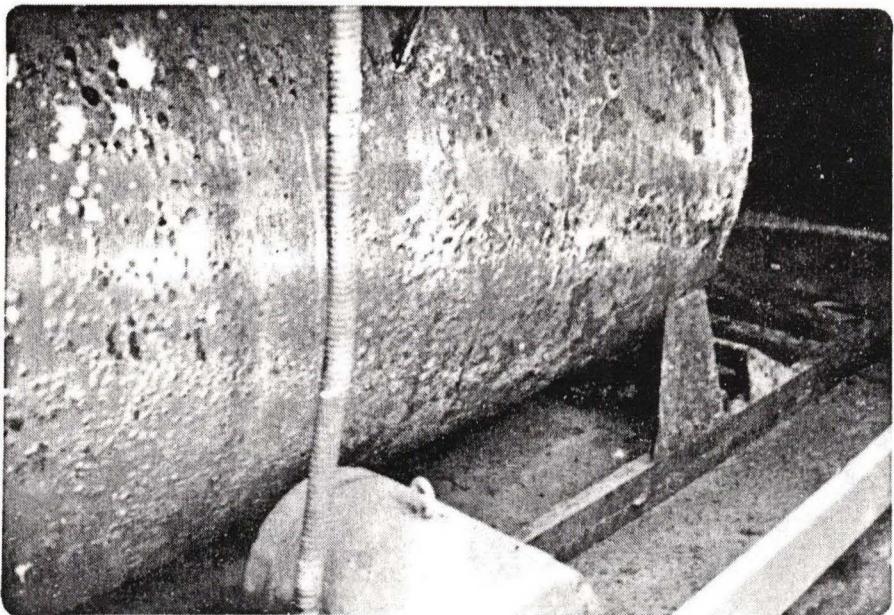
Figure 14 - Typical Coating Deterioration On
Fire Retardant Mixing Plant
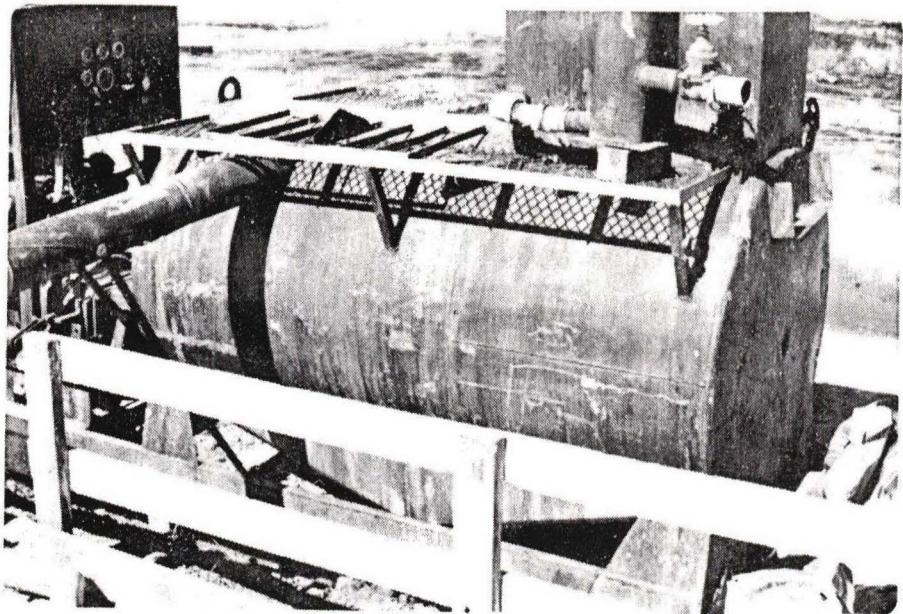
Figure 15 - Typical Coating Deterioration On
Fire Retardant Mixing Plant
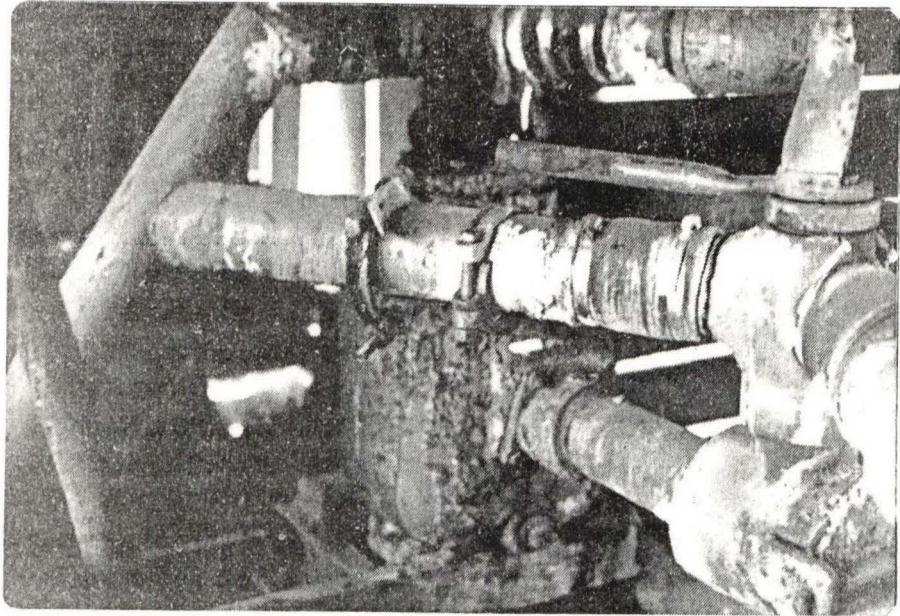
Figure 16 - External Corrosion and Coating
Deterioration On Fire Retardant Pump
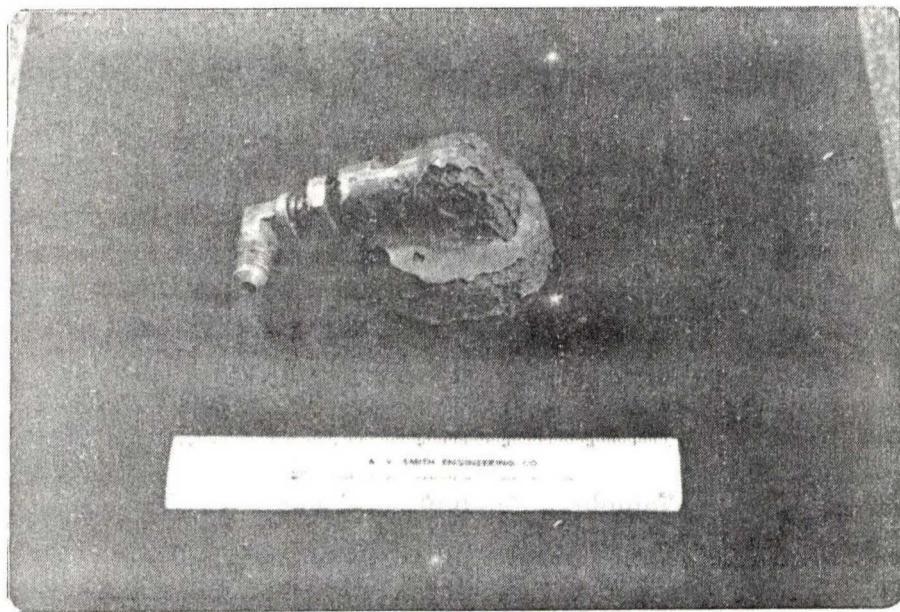
Figure 17 - Severe Pitting Corrosion On Hydraulic
Cylinder Cap Made From Magnesium

304 STAINLESS STEEL
410 STAINLESS STEEL
NAVAL BRASS
4130 STEEL
MAGNESIUM
6061 AL
7075 AL
2024 ALCLAD AL
2024 AL
ZINC

////// Weight loss
█████ Polarization

.001   .01   .1   1   10

Corrosion rate, MPY

FIGURE 18 – GENERAL CORROSION RATES IN PHOS–CHEK XA

-89-

FIGURE 19 – GENERAL CORROSION RATES IN PHOS–CHEK 259
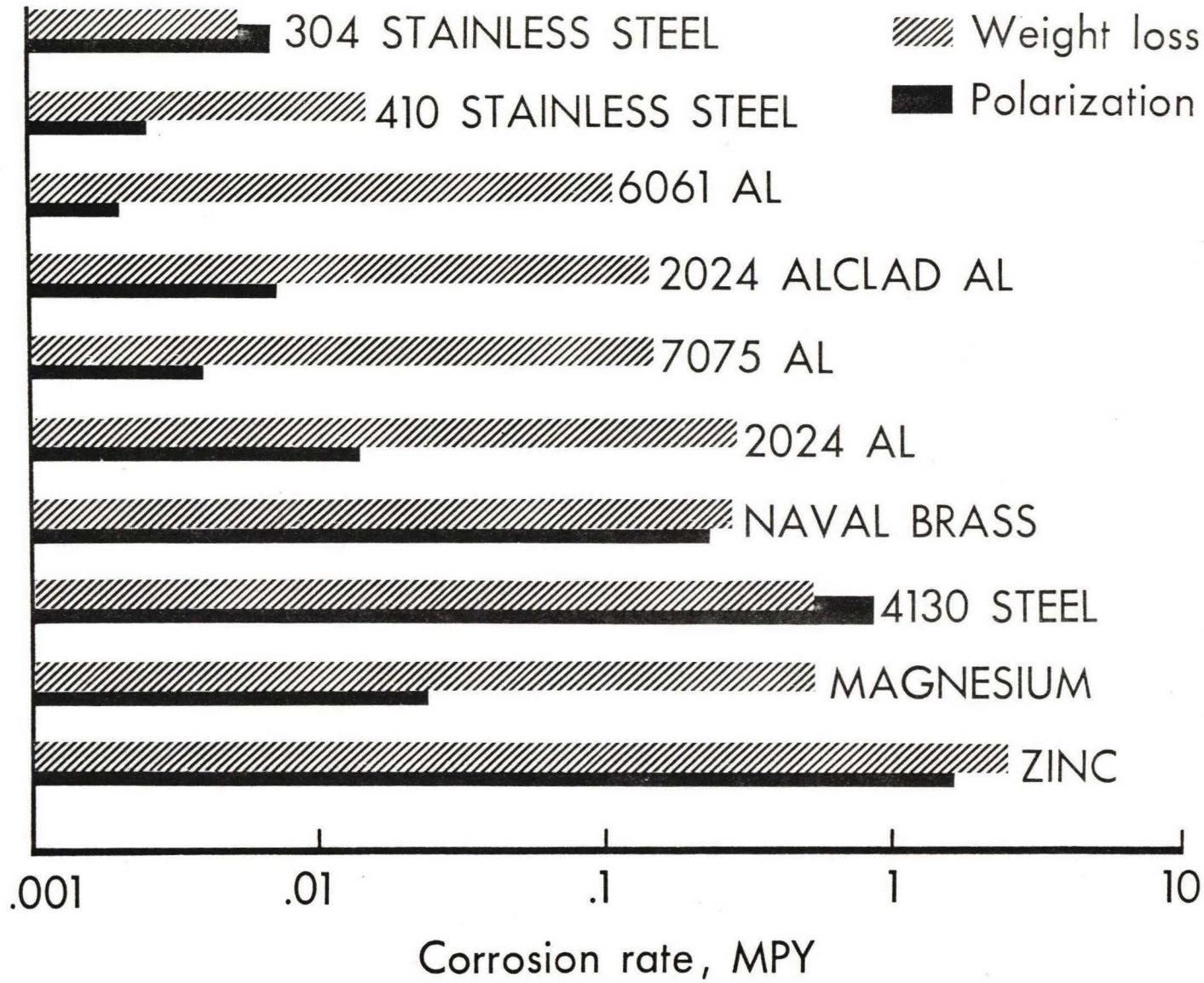
FIGURE 20 – GENERAL CORROSION RATES IN FIRE-TROL 931

410 STAINLESS STEEL

304 STAINLESS STEEL

4130 STEEL

NAVAL BRASS

6061 AL

2024 ALCLAD AL

7075 AL

2024 AL

ZINC

MAGNESIUM

Weight loss

Polarization

Corrosion rate, MPY

-91-
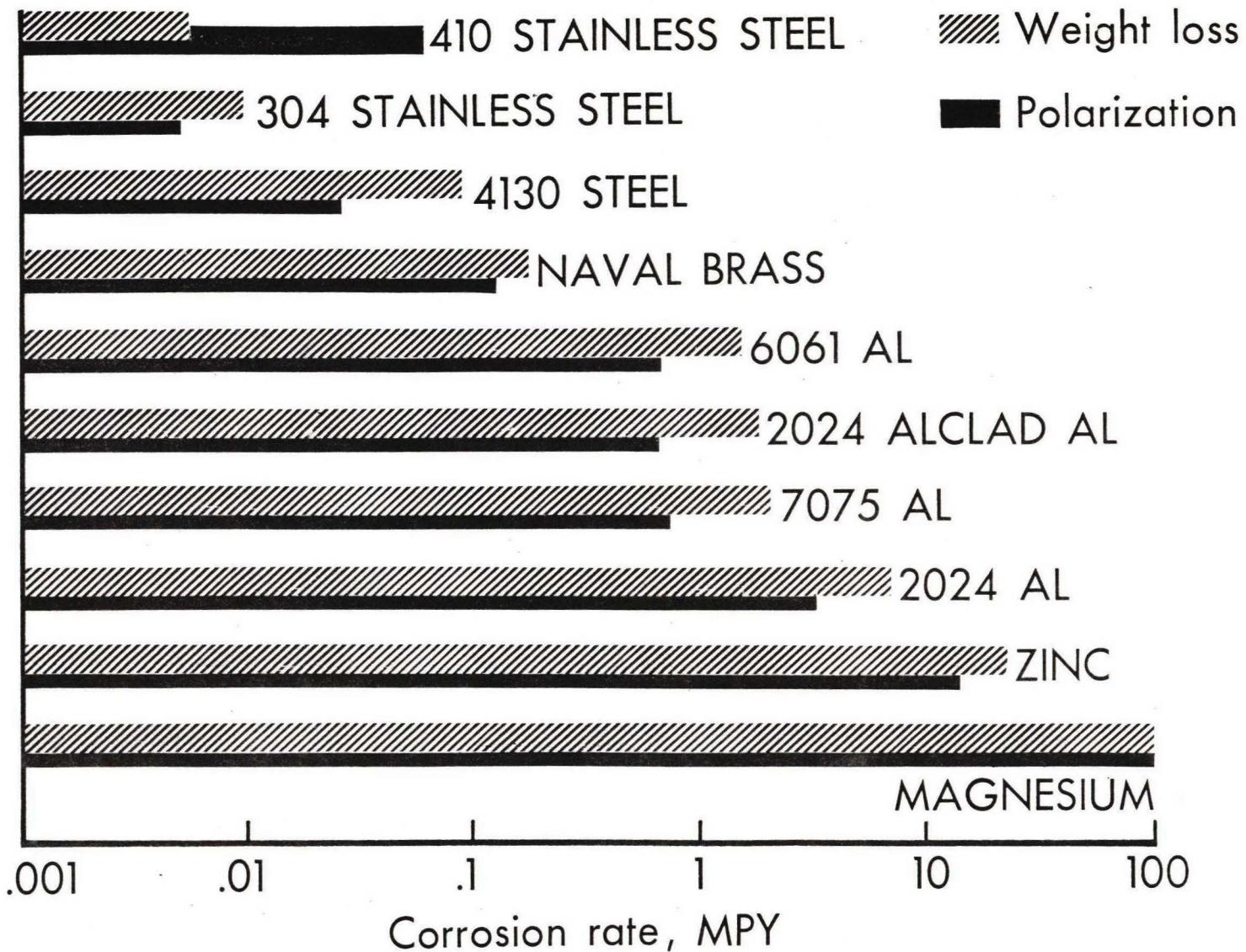
FIGURE 21 - GENERAL CORROSION RATES IN FIRE-TROL 100
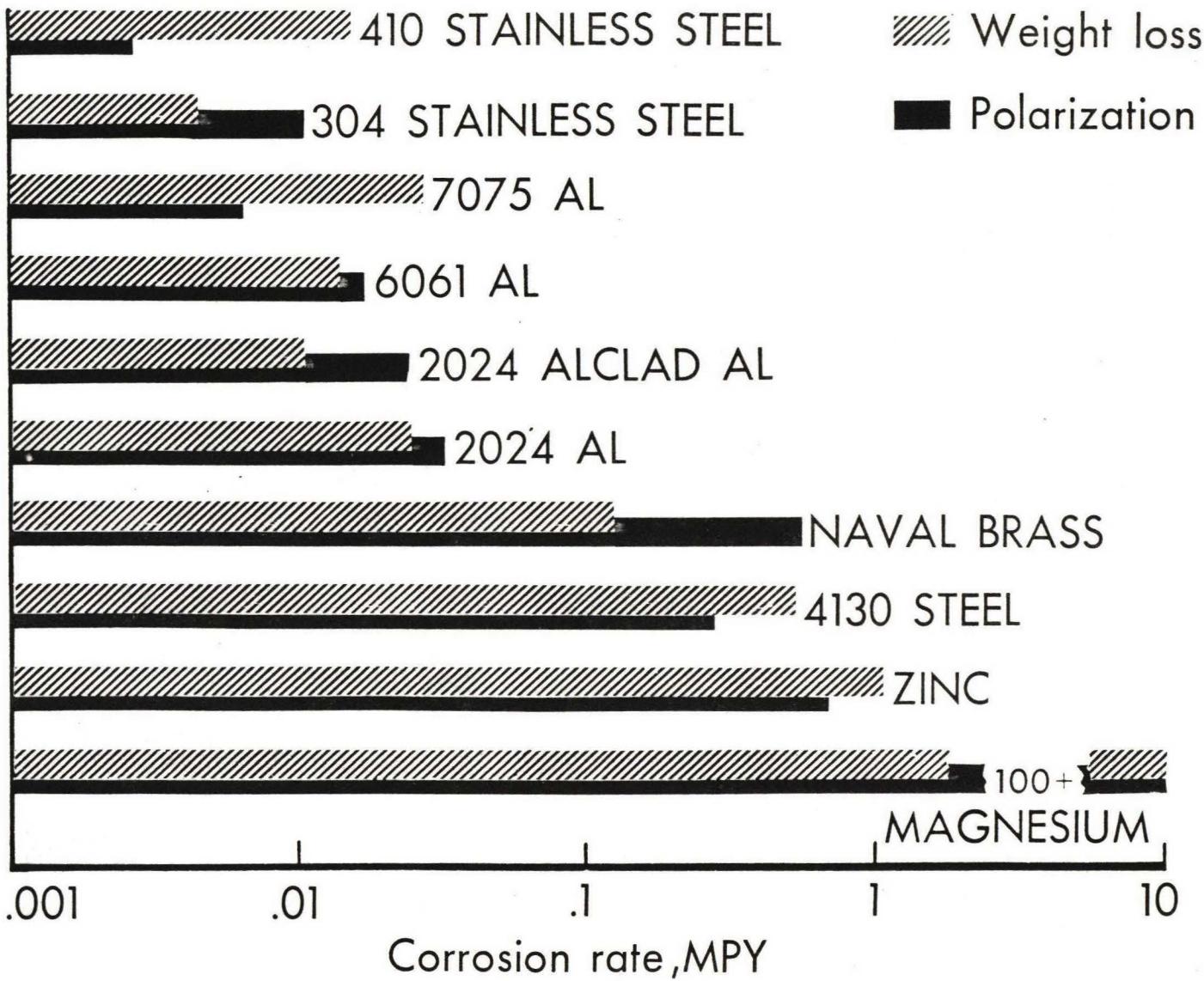
FIGURE 22 - GENERAL CORROSION RATES IN PYRO
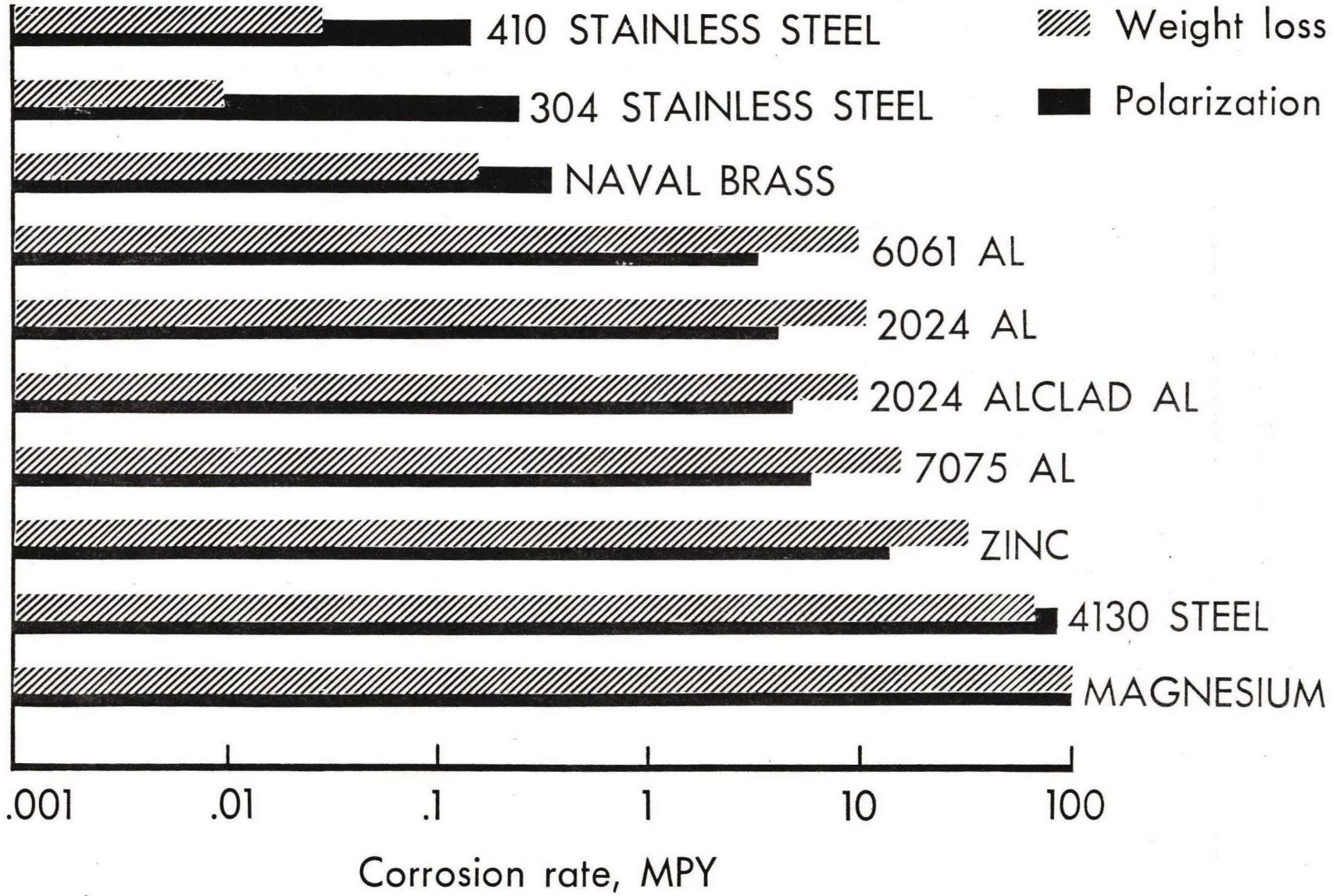
FIGURE 23 – Calculation of Galvanic Corrosion Rate for 7075 Al – 4130 Stl Couple in Pyro

$\Delta E_C = .030$ volts

7075 AL

4130 STEEL

$I_C = 13\ \mu$ amp/cm^2

Corrosion rate = 5.68 mpy

Potential = volts

Applied current density, μ amps/cm^2

.1   1   10   100
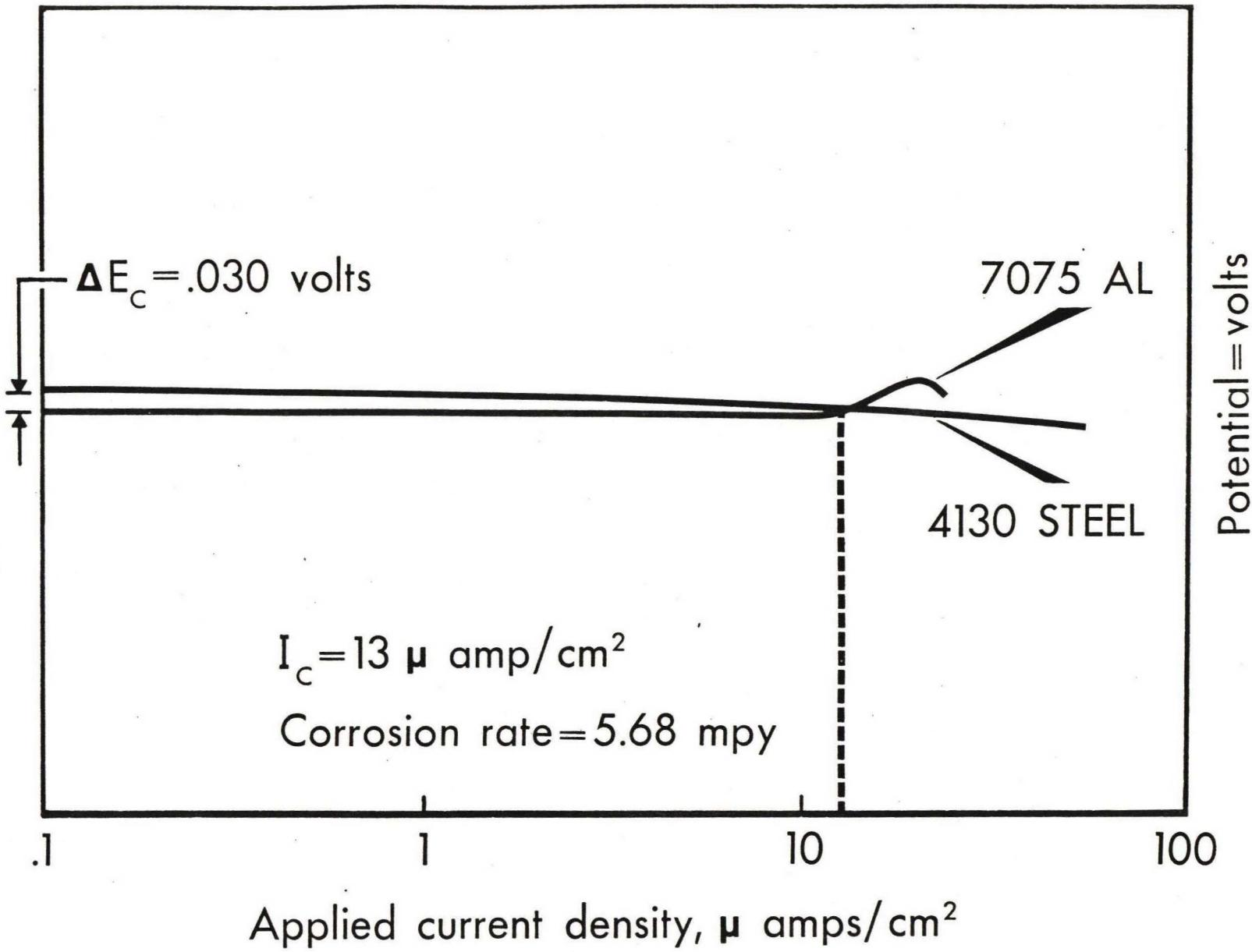
FIGURE 24 - Calculation of Galvanic Corrosion Rate for
7075 Al - 4130 Stl Couple in Fire-Trol 931
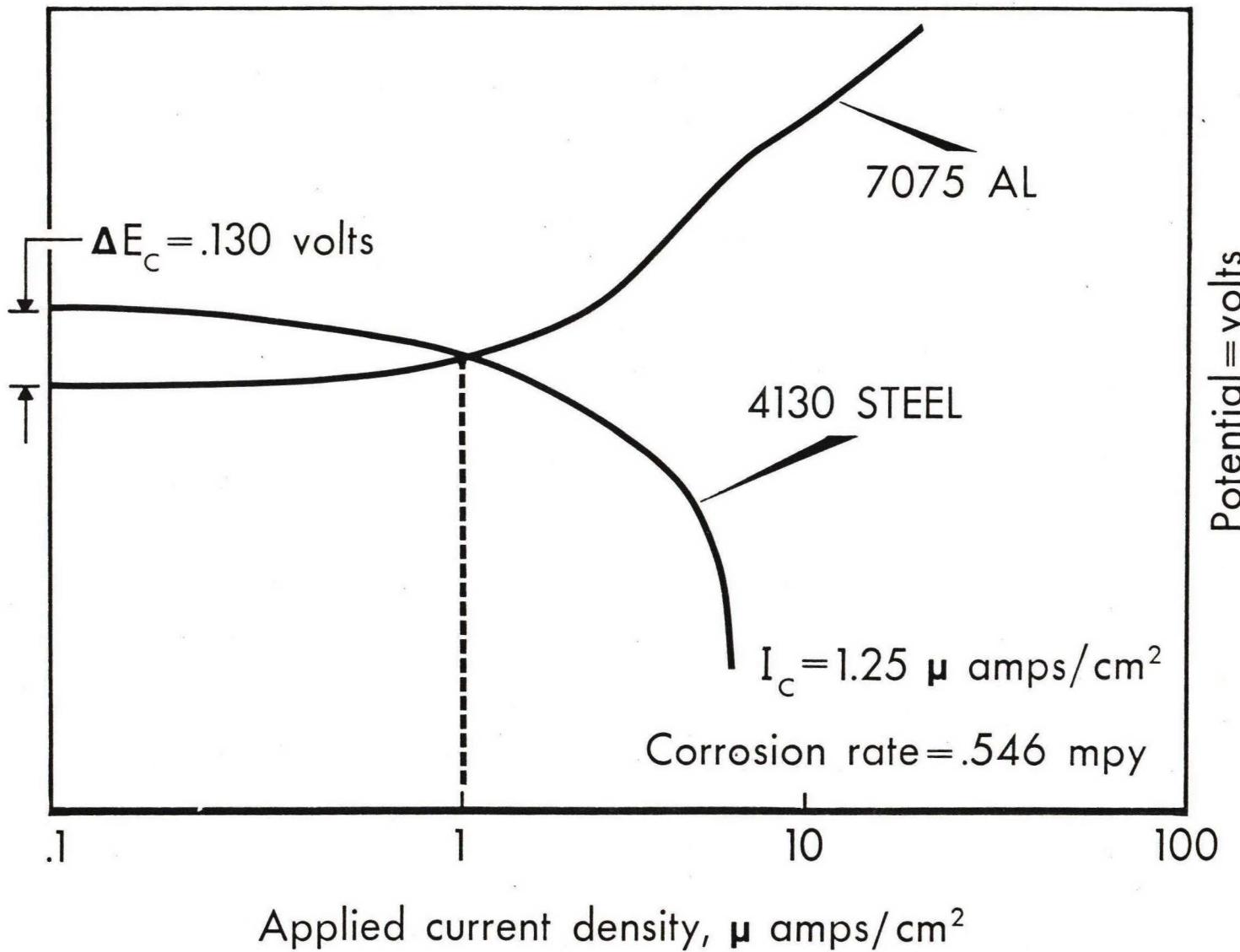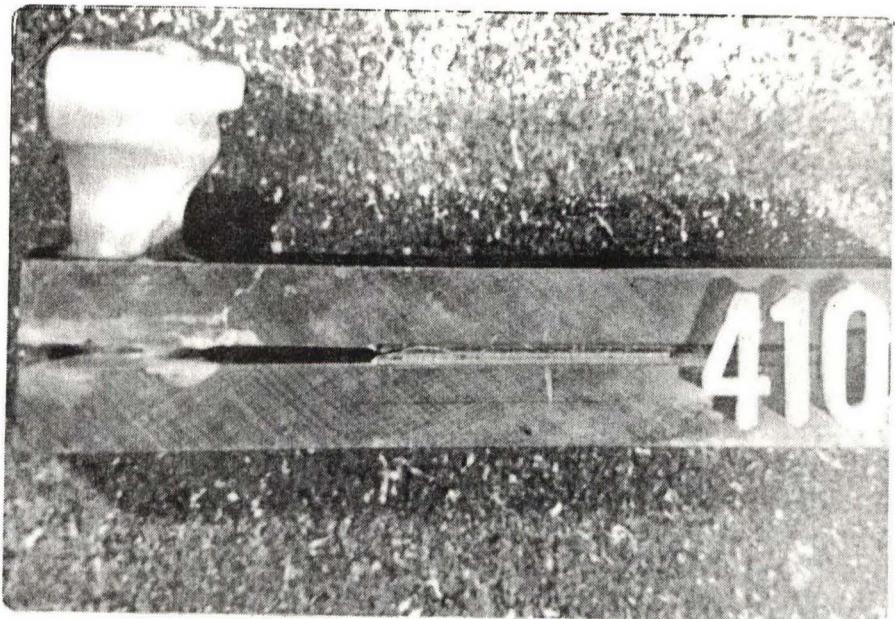
Figure 25 - DCB Specimen After Exposure to
Fire Retardant
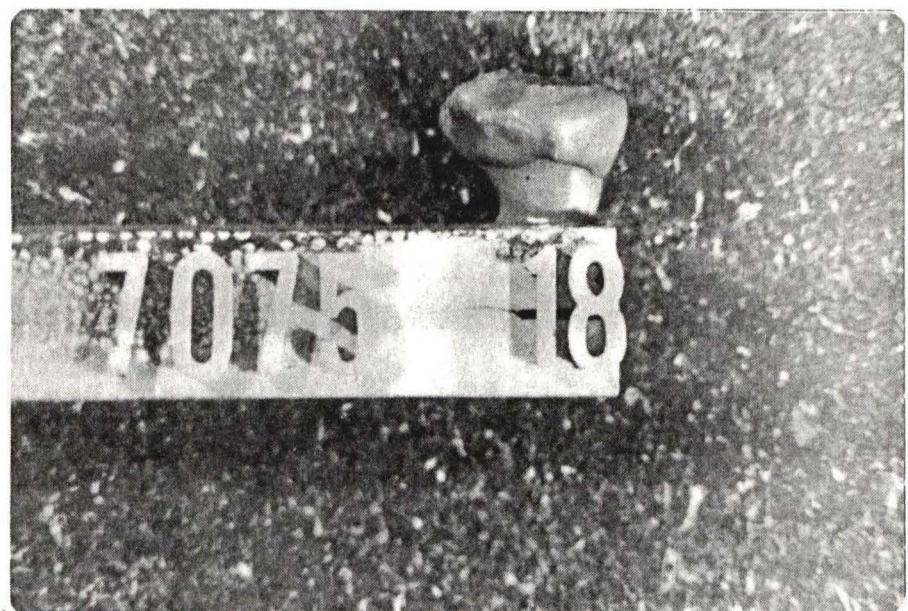
Figure 26 - DCB Specimen After Exposure to
Fire Retardant
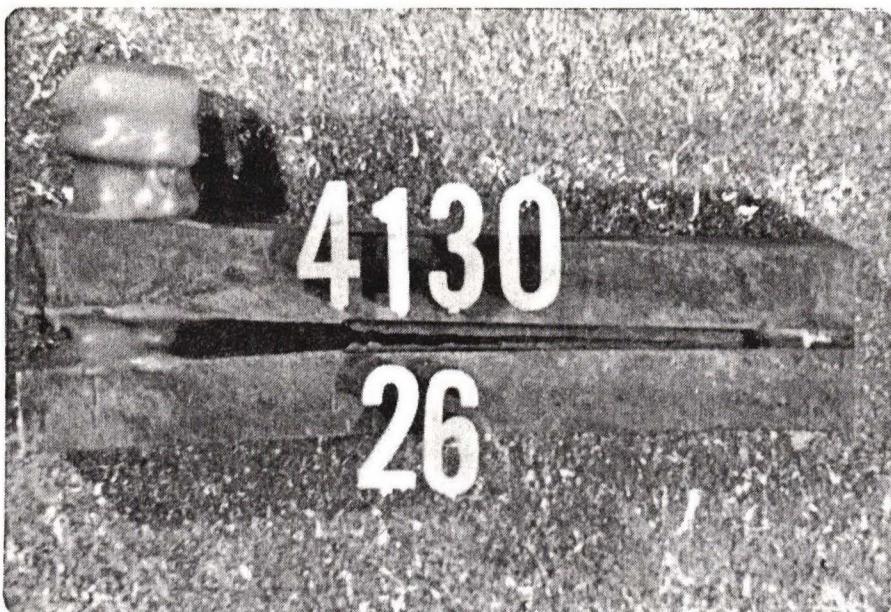
Figure 27 - DCB Specimen After Exposure to
Fire Retardant

FIGURE 28 — Fatigue Plots for 2024-T3 Aluminum in air and fire retardants

Legend:
- ● AIR
- ○ PYRO
- □ PHOSCHEK XA
- ◇ FIRETROL 931-L
- ▲ FIRETROL 100
- ◇ PHOSCHEK 259

→ indicates no failure at this point.

Stress (psi × 1000)

Cycles to failure
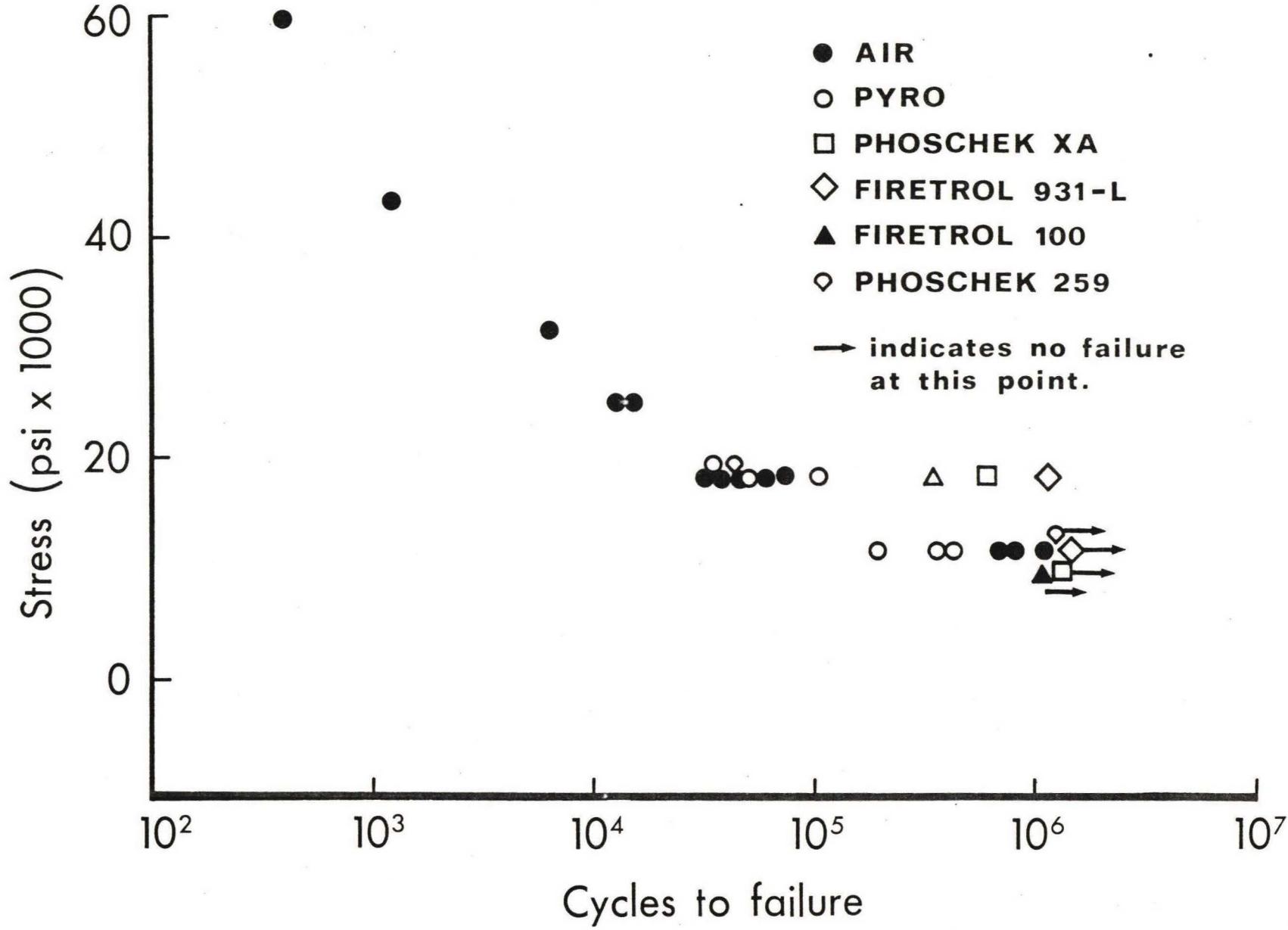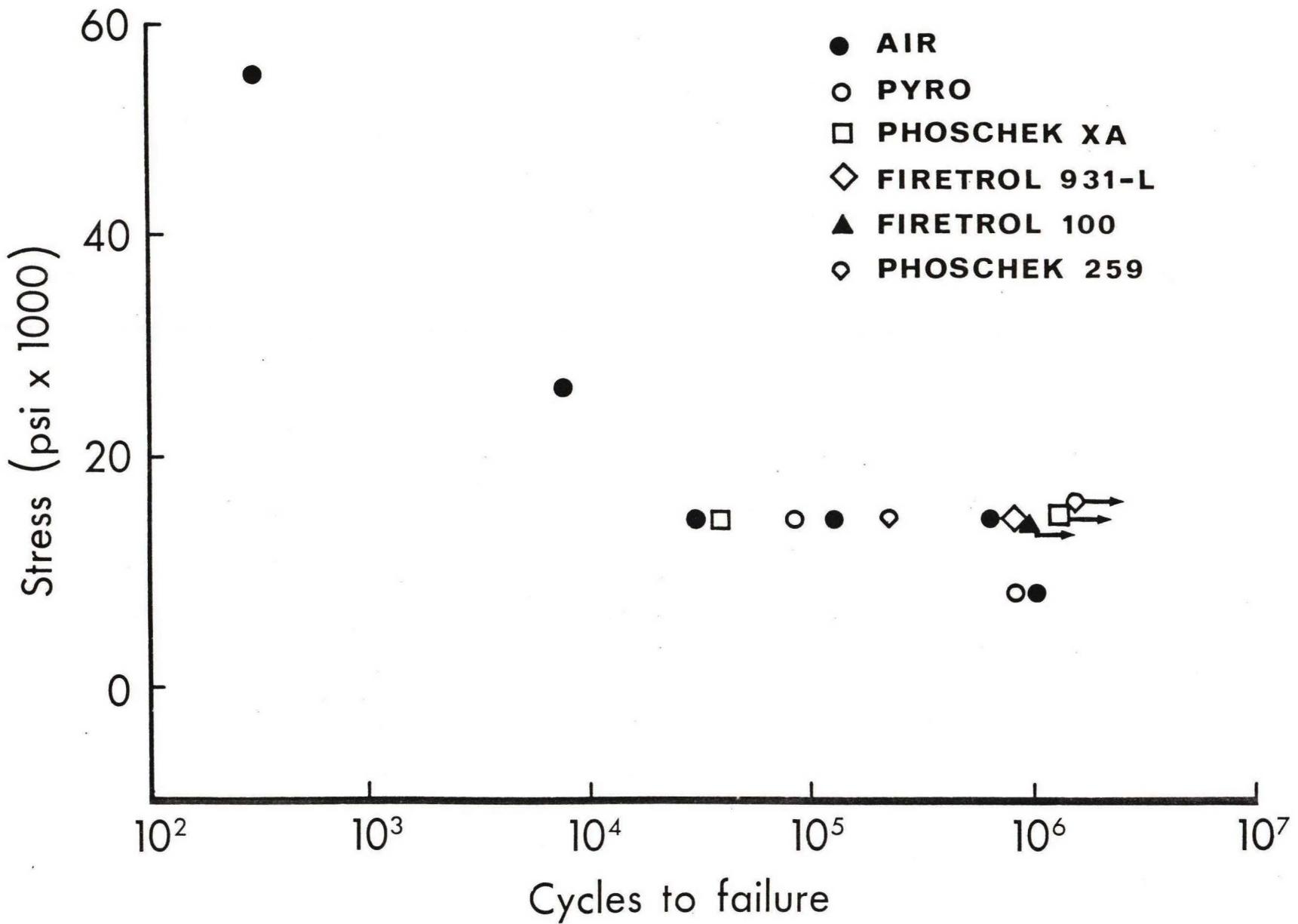
FIGURE 29 — Fatigue Plots for 7075-T6 Aluminum in air and fire retardants
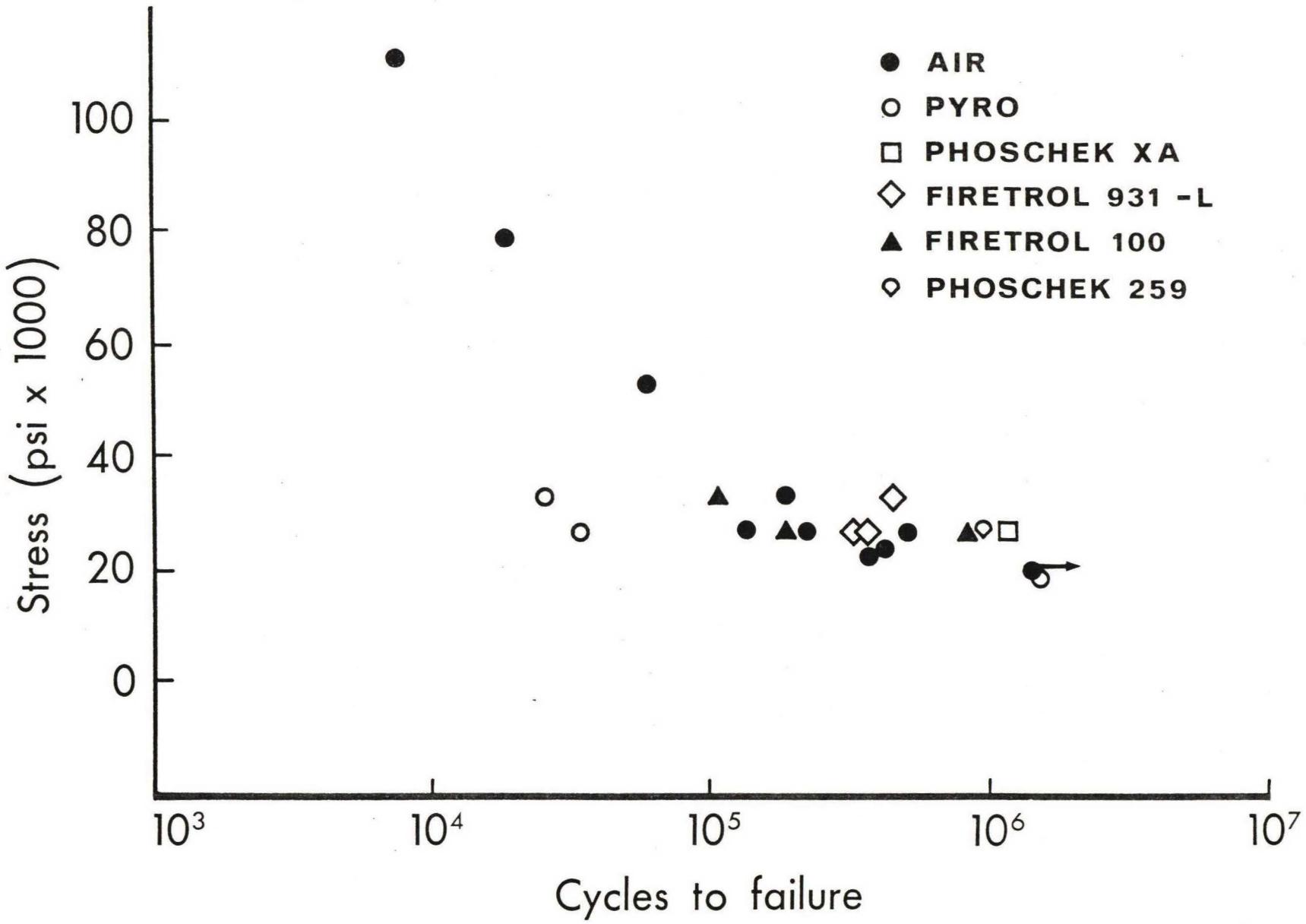
FIGURE 30 – Fatigue Plots for 4130 Steel in air and fire retardants

Figure 31 - DCB Specimen After Exposure to
Fire Retardant

FIGURE 32 – Effective Coating Thickness Versus Time in Diammonium Phosphate

Legend:
- ○ MODIFIED-OIL ALKYD
- □ EPOXY- POLYAMIDE
- ▼ EPOXY- AMINE
- △ EPOXY- COAL TAR
- ▽ EPOXY- ESTER
- ▷ MODIFIED ACRYLIC
- ◁ ACRYLIC LATEX
- ● PHENOLIC
- ■ FLAKE- FILLED POLYESTER
- ▲ BITUMINOUS ASPHALTIC EPOXY
- ◀ VINYL

Y-axis: Coating thickness (mils)
X-axis: Time (days)
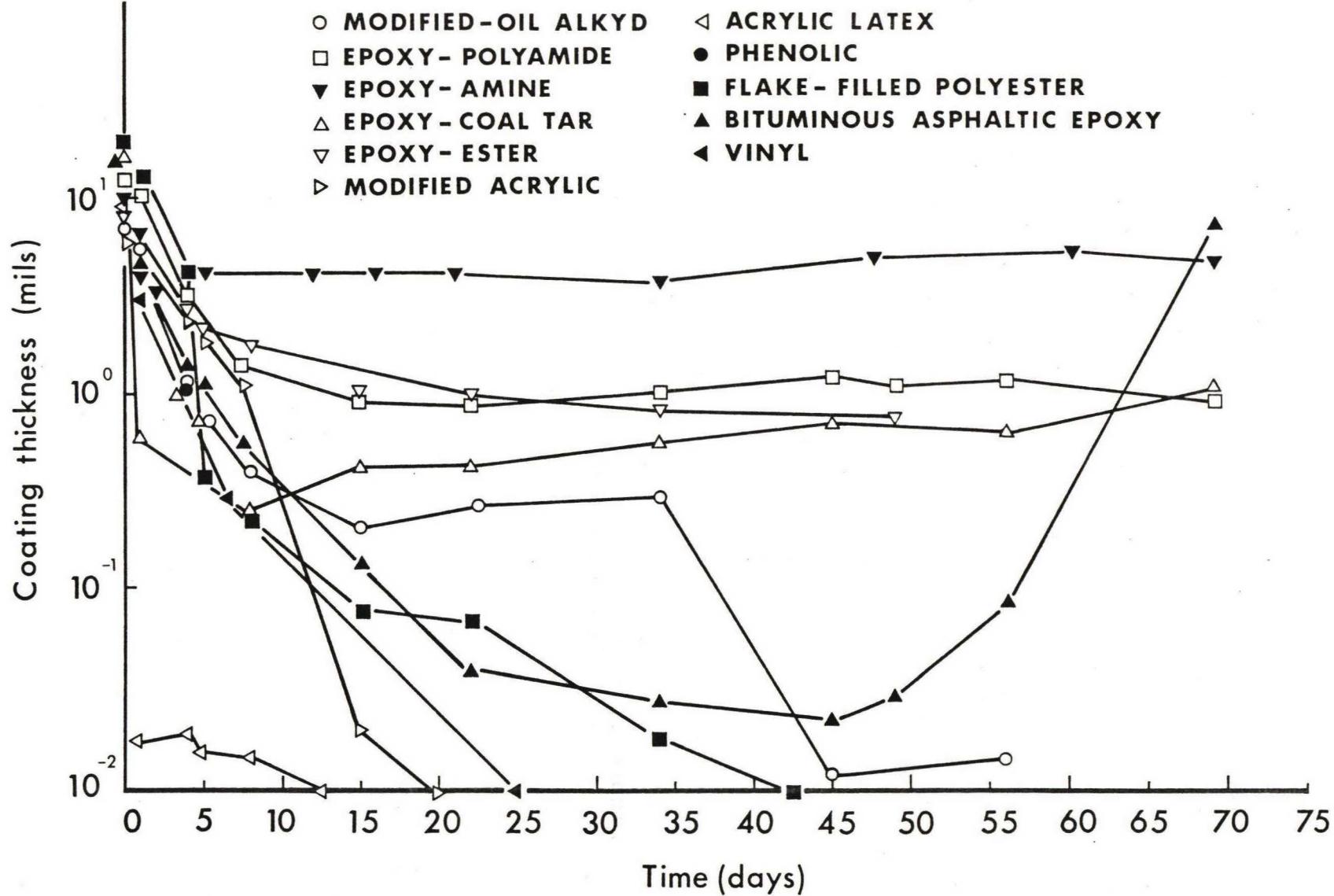
FIGURE 33 – Effective Coating Thickness Versus Time in Ammonium Sulphate

-103-

Legend:
○ MODIFIED-OIL ALKYD
□ EPOXY-POLYAMIDE
▼ EPOXY-AMINE
△ EPOXY-COAL TAR
▽ EPOXY-ESTER
▷ MODIFIED ACRYLIC
◁ ACRYLIC LATEX
● PHENOLIC
■ FLAKE-FILLED POLYESTER
▲ BITUMINOUS ASPHALTIC EPOXY
◀ VINYL

Coating thickness (mils)

Time (days)
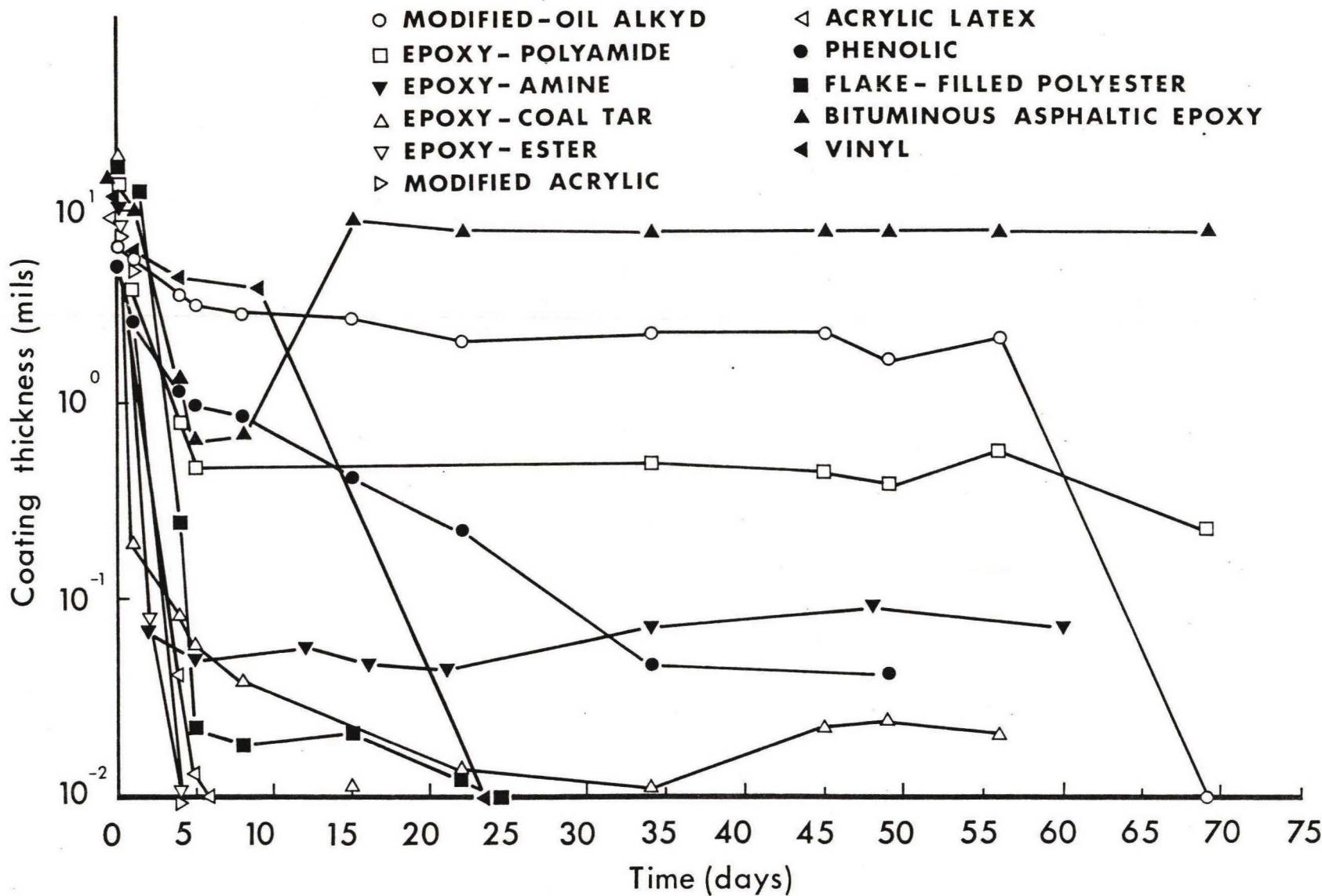
FIGURE 34 – Effective Coating Thickness Versus Time in Pyro
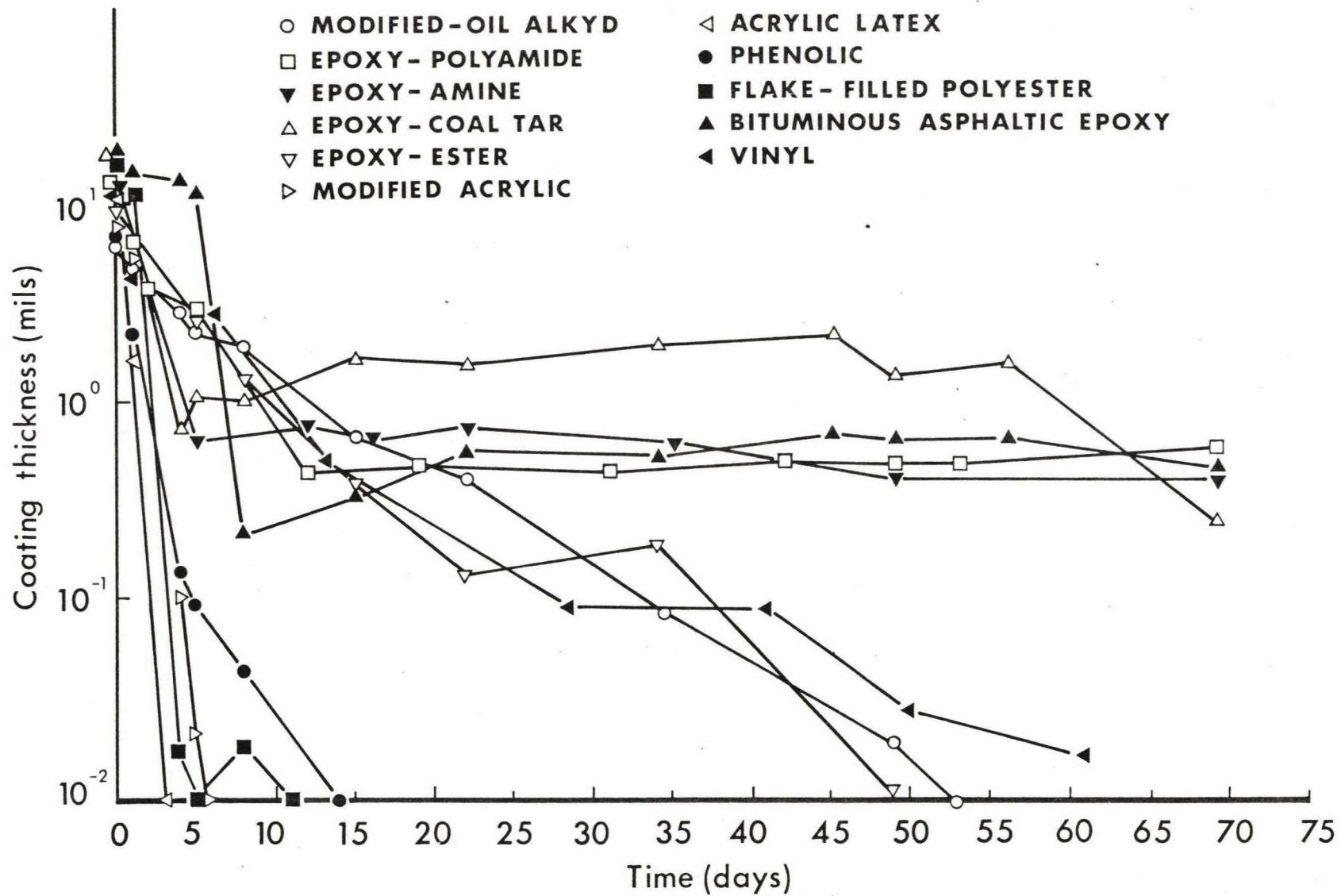
FIGURE 35 – Resistance Versus Time in Diammonium Phosphate

Legend:
- ○ MODIFIED-OIL ALKYD
- □ EPOXY- POLYAMIDE
- ▼ EPOXY- AMINE
- △ EPOXY- COAL TAR
- ▽ EPOXY- ESTER
- ▷ MODIFIED ACRYLIC
- ◁ ACRYLIC LATEX
- ● PHENOLIC
- ■ FLAKE- FILLED POLYESTER
- ▲ BITUMINOUS ASPHALTIC EPOXY
- ◀ VINYL

Resistance (ohms) vs Time (days)
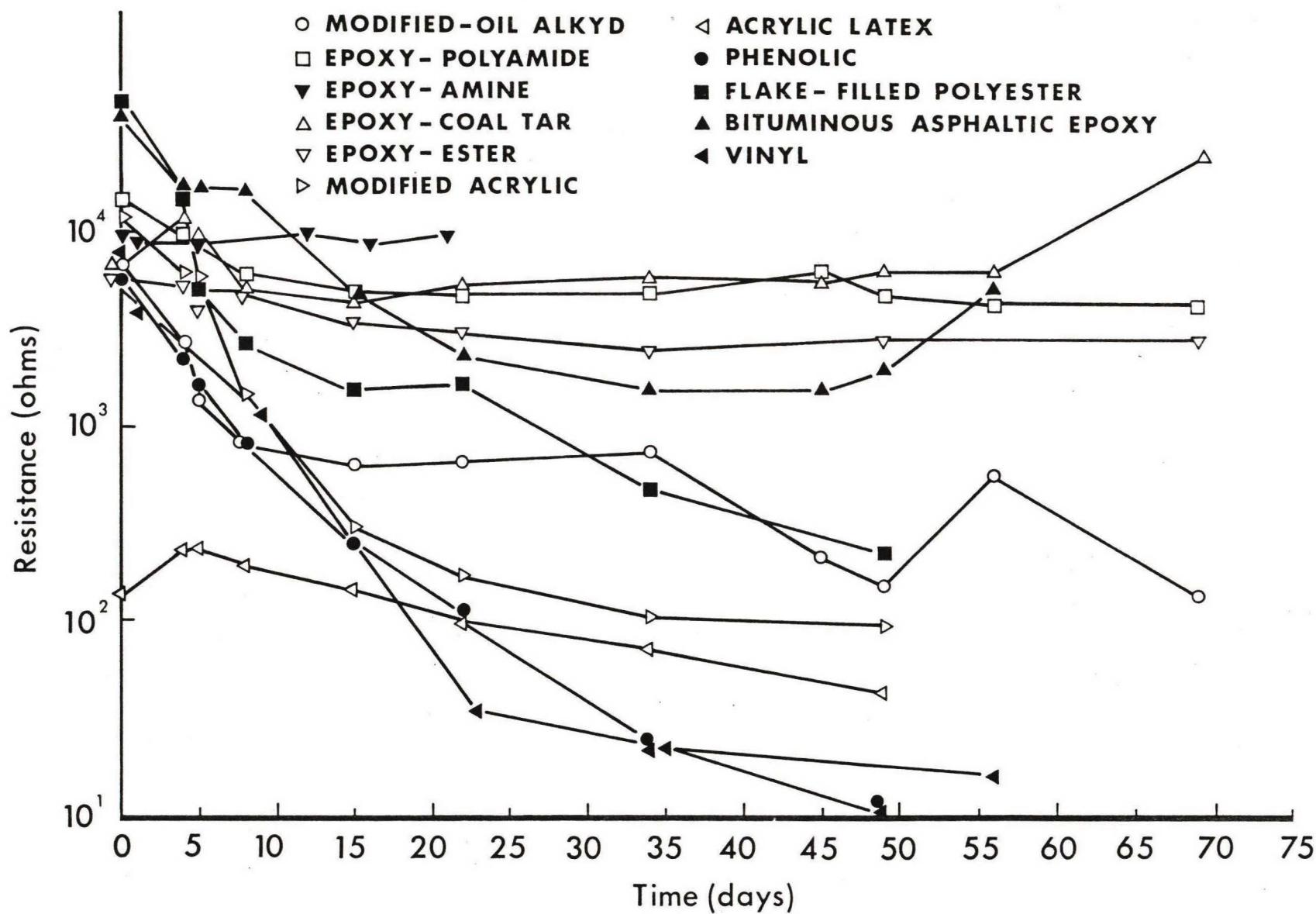
FIGURE 36 – Resistance Versus Time in Ammonium Sulphate

-106-
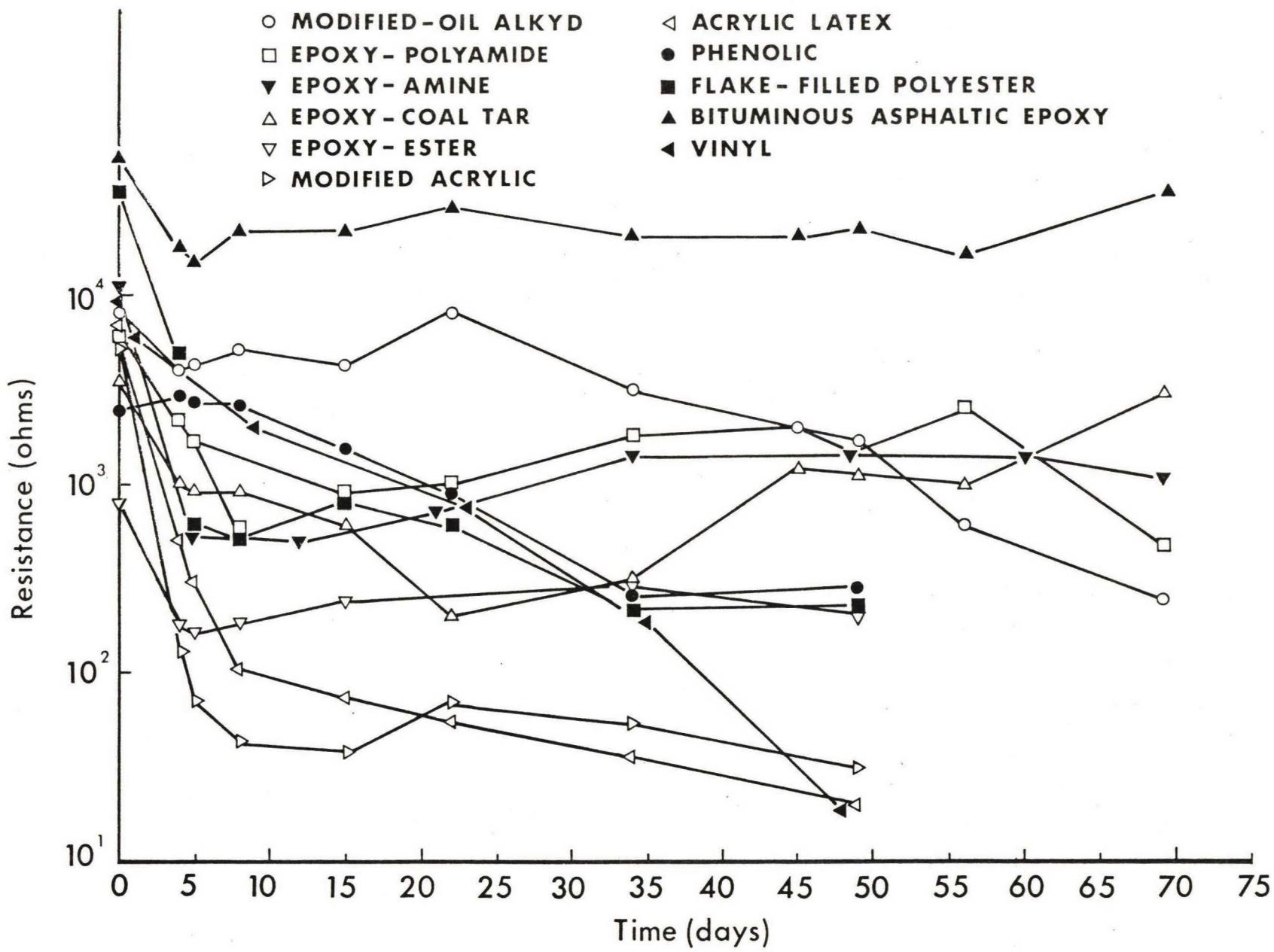
FIGURE 37 - Resistance Versus Time in Pyro

Legend:

○ MODIFIED-OIL ALKYD
□ EPOXY- POLYAMIDE
▼ EPOXY- AMINE
△ EPOXY- COAL TAR
▽ EPOXY- ESTER
▷ MODIFIED ACRYLIC
◁ ACRYLIC LATEX
● PHENOLIC
■ FLAKE- FILLED POLYESTER
▲ BITUMINOUS ASPHALTIC EPOXY
◀ VINYL

Resistance (ohms)

Time (days)
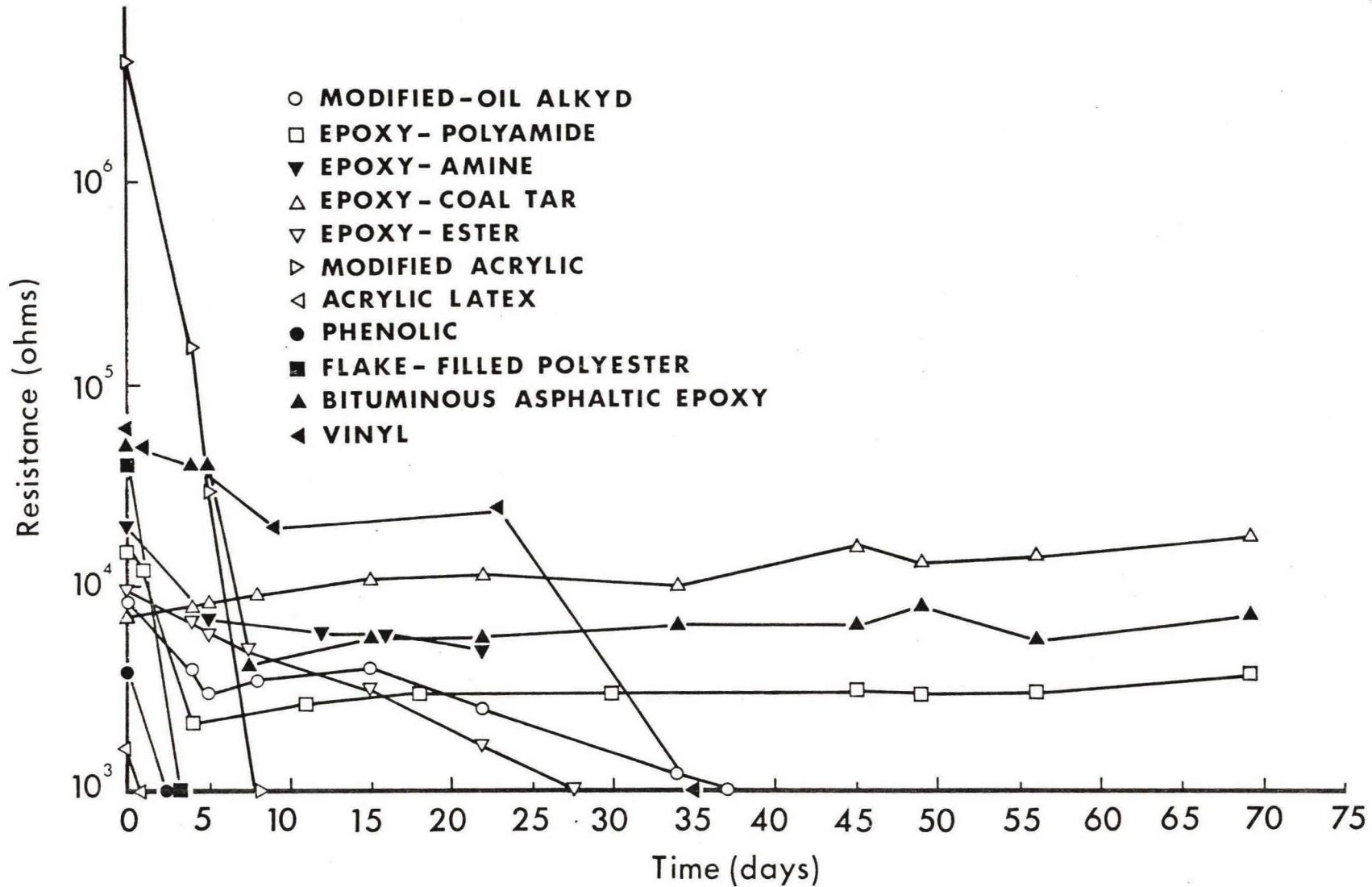
Appendix I - Air Tankers and Mixing Plants
Inspected During Field Survey

A. Aircraft

Type		Identification No.
1.	TBM	A-14, N3249 G
2.	TBM	A-6, N9597 C
3.	B-26	A-17, N3426 G
4.	TBM	A-22, N7157 C
5.	TBM	A-27, N7017 C
6.	B-17	C-10, N66573
7.	B-17	B-30, N932
8.	PB4Y2	A-25, N6313 D
9.	B-17	A-18, N66571
10.	TBM	A-12, N6824 C
11.	TBM	A-13, N9010 C
12.	TBM	A-7, N7015 C
13.	P2V	A-15, N14448
14.	TBM	A-21, N3969 A
15.	P2V	H-1, N1262
16.	PV2	37, N6657 D
17.	PV2	40, N6651 D
18.	PV2	43F, N7086 C
19.	B-26	74F, N74874
20.	PBY	B27, N6884 C
21.	DC-6	82, N37515
22.	PBY	B-23, N7620 C
23.	B-26	A-28, N3427 G
24.	PB4Y	B-24, N2872 G
25.	B-26	D27, N9403 Z
26.	C-119	12, N13743
27.	C-119	N8682
28.	DC-6B	02, N660 G
29.	B-17	18, N5233 V
30.	DC-6	84, N37565
31.	DC-6	85, N37585
32.	B-26	44, N9682 C
33.	B-26	18, N9159 Z
34.	AF	30E, N3144 G
35.	C-119	13, N13744
36.	B-17	19C, N5230 V
37.	DC-6	16, N37574
38.	AF	21E, N9995 Z
39.	F7F	43E, N6178 C
40.	F7F	42E, N7626 C
41.	F7F	41E, N7629 C
42.	F7F	31E, N6177 C
43.	Super PBY	49E, N2886 D
44.	TBM	27E, N1369 N
45.	TBM	26E, N9078 Z

46.	TBM	68,	N5168 V
47.	Super PBY	84E,	N6456 C
48.	Super PBY	83E,	N6458 C
49.	TBM	72E,	N3357 G
50.	TBM	52E,	N9434 Z
51.	Super PBY	54E,	N6453 C
52.	B-17	71C,	N809 Z
53.	F7F	63E,	N7654 C
54.	F7F	62E,	N6129 C
55.	TBM	74E,	N7833 C
56.	TBM	97E,	N7161 C
57.	TBM	58E,	N6827 C
58.	F7F	64E,	N7235 C
59.	F7F	23E,	N6179 C
60.	B-17	78E,	N3703 G
61.	TBM	25E,	N68663
62.	TBM	24E,	N7961 C

B. Mixing Plants

1. Missoula, Montana
2. Kalispel, Montana
3. Helena, Montana
4. West Yellowstone, Wyoming
5. Cody, Wyoming
6. Dour D'Alene, Idaho
7. Grangeville, Idaho
8. Wenatchee, Washington
9. LaGrande, Oregon
10. Boise, Idaho
11. Redding, California
12. Redmond, Oregon
13. Medford, Oregon
14. Montague, California
15. Chester, California
16. Chico, California
17. Willows, California
18. Grass Valley, California
19. Ukiah, California
20. Sonoma County, California (Santa Rosa)
21. Columbia County, California (Sonora)
22. Romona, California
23. Ryan Field, Hemet, California
24. Goleta, California
25. Paso Robles, California
26. Porterville, California
27. Fresno, California
28. Hollister, California

APPENDIX II

THE USE OF ELECTROCHEMICAL POLARIZATION TECHNIQUES
TO MEASURE CORROSION RATES

Advances in electrochemistry in recent years have evolved test techniques that overcome some of the limitations of simple weight loss measurements. Several techniques utilizing electrochemical measurements are now available to determine the corrosion rate of a metal exposed to a corrosive electrolyte.

When a metal is in a state of reversible equilibrium with a solution of its ions, simultaneous oxidation and reduction reactions are taking place with no net change in the weight of the metal electrode or the concentration of ions. The rate of oxidation and reduction taking place can be expressed in terms of Faraday's Law:

$$(1) \quad r_{ox} = r_{red} = i_o/nF$$

Where i_o is called the exchange current. Since oxidation current and reduction current have opposite polarities, at equilibrium there is no net current.

When the equilibrium of an electrode reaction is disturbed, there is a change in the potential of the electrode when measured against a stable reference. The difference between the equilibrium potential and the potential under the new conditions is called polarization and is usually designated by the Greek letter Eta, η. Mathematically:

$$(2) \quad \eta = E_{eq} - E$$

Where E_{eq} is the potential at equilibrium and E is the potential under the new conditions. Disturbance of the equilibrium condition alters the exchange current balance and results in a net current flow, either oxidation or reduction, which is representative of the net rate of reaction. Polarization, therefore, results from any situation involving a net current flow to or from an electrode surface.

A metal undergoing corrosion involves two reactions, one at the cathode and one at the anode. Because of the current flow between local cathodes and anodes, a corroding metal polarizes toward a common potential, E_{cor}. The behavior of the corroding metal is studied by application of an external current. A measured and externally controlled source of direct current is connected between the corroding metal and a counter electrode. The change in potential (polarization) of the corroding metal is then determined as a function of the externally applied current, either anodic or cathodic.

The "linear" polarization technique for determining corrosion rates involves polarizing a test specimen $\pm$ 20 millivolts from the corrosion potential and measuring the currents associated with this partial polarization curve. Early researchers[1] thought that a linear relation existed between current and potential. They hypothesized that the slope of this "linear" polarization curve was inversely proportional to the corrosion rate according to the following expression:

$$(3) \quad \frac{\Delta E}{\Delta I} = \frac{1}{2.3} \times \frac{\beta a \times \beta c}{\beta a + \beta c} \times \frac{1}{I_c}$$

Where I_c = corrosion current density

β_a = Anodic Tafel Slope

β_c = Cathodic Tafel Slope

ΔI = Impressed Current Density

ΔE = Polarization caused by impressed current when ΔE < 20 millivolts

The corrosion rate is a linear function of I_c according to Faraday's Law:

$$\text{corrosion rate} = \frac{kI_c}{\rho}$$

where k = electrochemical equivalent for specific metal

ρ = density of specific

Recent work by Mansfeld[2], however, demonstrates that there is no theoretical justification for polarization curves to be linear at or within $\pm$ 20 millivolts of the corrosion potential. He shows, in fact, that non-linearity is severe in many cases. This does not void, however, this polarization technique for determining corrosion rates. Mansfeld shows that with some modification of data analysis, polarization curves within $\pm$ 20 millivolts of the corrosion potential can still be used as a basis for accurately calculating corrosion rates. The modifications include determination of $\frac{\Delta E}{\Delta I}$ @ I = 0 and application of curve fitting techniques to more precisely determine β_a and β_c. The formula hypothesized by Stern is then shown to be valid.

[1] M. Stern and A. L. Geary, "Electrochemical Polarization - Part 1, "Inl. Electrochem. Soc., 104, (1957).

[2] F. Mansfeld, "Electrochemical Background of the Polarization Resistance Technique", a paper presented at the NACE Corrosion Conference, 1973.

Appendix III - Prediction of Galvanic Corrosion Rates

From Electrochemical Potential and

Polarization Measurements

Galvanic corrosion occurs because of a difference
in corrosion potential existing between two dissimilar
metals that are in contact with each other and exposed to
the same corrodent. The alloy exhibiting a more active
potential will corrode. The other alloy will, in effect,
be under cathodic protection.

The rate of galvanic corrosion is determined by
the potential difference between the dissimilar metals and
the polarization characteristics of each metal. The theo-
retical aspects of electrochemical polarization were dis-
cussed in Appendix II.

To evaluate the relative tendency for galvanic
corrosion to occur in fire retardants, potential and polar-
ization data were obtained for ten (10) alloys in five (5)
fire retardants. Using this data, a galvanic corrosion
rate can be estimated for any two dissimilar alloys in any
retardant. The techniques involved are best illustrated by
considering a specific example.

Consider equal areas of 2024 Aluminum and Naval Brass coupled directly in Phos-Chek XA. Since the aluminum alloy is more active (-.86 volts), it will corrode. The brass alloy @ -.34 volts will be under cathodic protection. The potential difference for this couple is .52 volts. This is the driving force of the rate reaction. The polarization characteristics, however, will control the actual rate.

By simultaneously plotting the anodic polarization curve in Phos-Chek XA for the aluminum alloy and the cathodic polarization curve for the brass alloy in Phos-Chek XA, a corrosion current can be determined. The galvanic corrosion current, I_c, is the point at which the two curves intercept, assuming no "IR" drop in the solution. This is a reasonable assumption in fire-retardants which exhibit electrical resistivities of $\simeq 10$ ohm-centimeters. The galvanic corrosion current in microamps / cm^2 is converted to more familiar units (mpy) using Faraday's law which relates current flow to weight loss. This calculation was described in Appendix II. Figure A-III-1 shows a plot of the polarization curves.
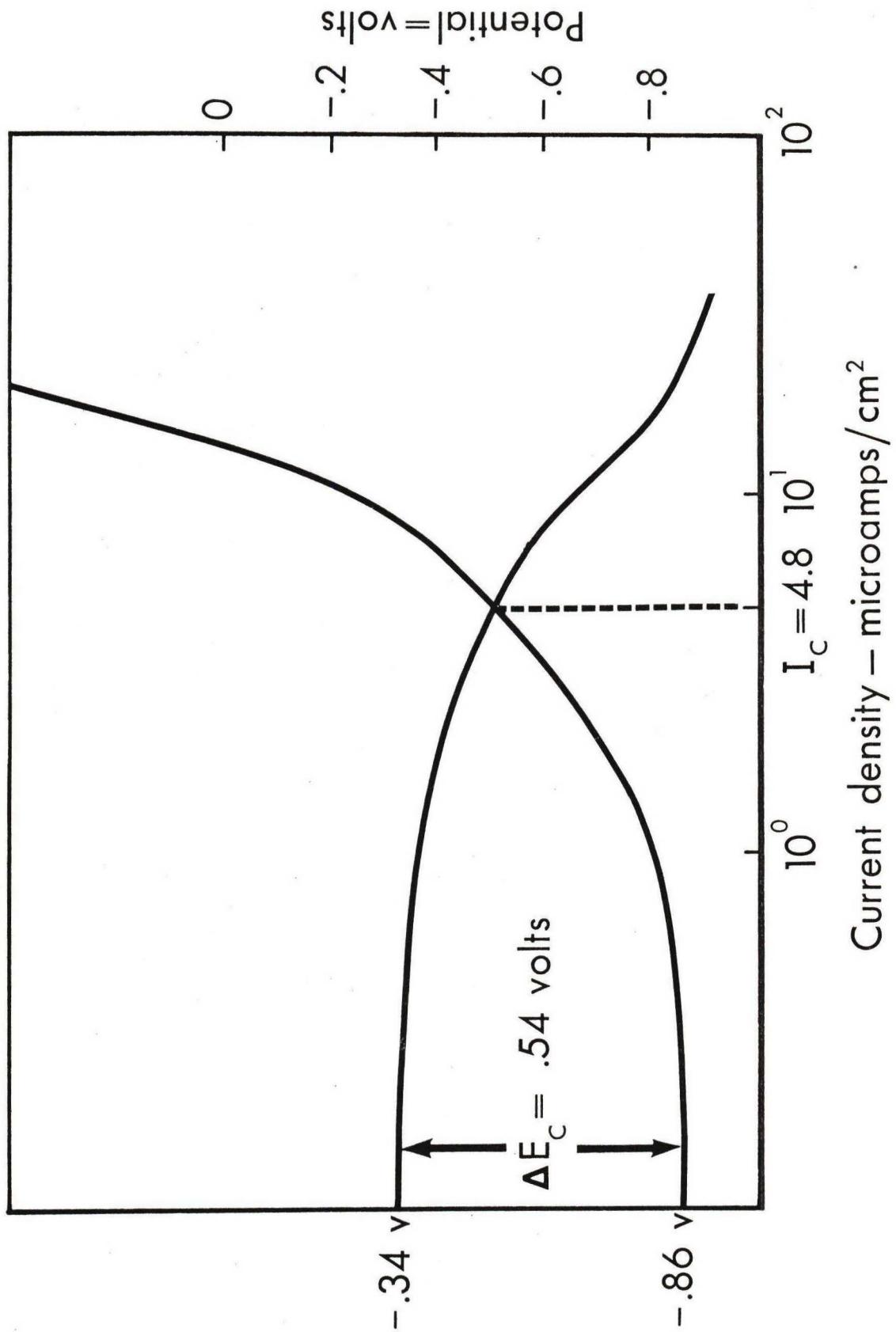
FIGURE A-III-I — Polarization plots for 2024 Aluminum (anodic) and Naval Brass (cathodic) in Phos-Chek XA

Appendix IV - Typical Corrosion Damage Observed
During Field Inspection Trips

A. Aircraft

  1. Shallow pitting (<10 mils) on interior surfaces
      of AlSl 1010 steel tanks and gates.

  2. Corrosion of brass cam arms on Kamlock cap.

  3. Significant corrosion of mild steel nuts and bolts
      on gate hinges and brackets.

  4. Corrosion of brass cable clamps on control cables.

  5. Isolated deep pitting on exterior of steel tanks.

  6. Light pitting ($\approx$5 mils) of aluminum tank, gate
      and torque tube.

  7. Significant pitting (10 to 40 mils) of steel tanks,
      gates, and fasteners.

  8. Light pitting on cast aluminum Kamlock fitting.

9. Significant pitting (5 to 20 mils) on aluminum gates, steel tanks, torque arms and torque tubes.

10. Exfoliation corrosion and pitting corrosion on aircraft skin.

11. Light corrosion of interior control cables near tank.

12. Corrosion of mild steel bands on rubber hoses.

13. Shallow pitting corrosion on aircraft fuselage.

14. Penetration of aircraft skin due to corrosion.

15. Pitting corrosion on mild steel fasteners and hinges.

16. Pitting corrosion on aluminum tanks.

17. Skin cracking, popped rivets, exfoliation and general corrosion back of tank.

18. Pitting of magnesium wheels.

19. Severe corrosion of bolts in tail area.

20. Perforation of skin in wheel well.

21. Severe corrosion of gate area, corrosion at seams to rear of tank, popped rivets.

22. Corrosion at seam near tail wheel, galvanic attack between aluminum and steel at reinforcing angles on doors.

23. Pitting of steel lubrication tubes, pitting on sections of fuselage to rear of tank, underfilm attack and corrosion at seam to rear of tank.

B. Ground-Mixing Equipment

1. Pitting and general corrosion of steel butterfly valve.

2. Blistering and deterioration of exterior paint coating on mixing and/or storage equipment.

3. General corrosion of brass valves.

4. General corrosion of brass fittings.

5. Significant general corrosion on interior of steel storage tank in retardant-air interface area.

6. Pitting corrosion on cast aluminum valves.

7. Pitting corrosion on wrought iron supply pipe.

8. Pitting corrosion on aluminum Kamlock fittings.

9. Pitting corrosion on brass pump seal.

10. Pitting corrosion of aluminum on LC retardant
    proportioner assembly.

11. Pitting corrosion on brass arm of flowmeter.

12. Significant coating degradation on interior of
    steel storage tank at retardant-air interface.

13. Roof cross member penetrated by corrosion, bolts
    on roof support completely corroded, corrosion on
    tank wall.

14. Paint blistering in storage tank vapor zone, joint
    leakage and under-film attack.